ACS Chemical Neuroscience

pubs.acs.org/chemneuro Research Article

Synthesis, Pharmacological, and Biological Evaluation of 2-Furoyl-Based MIF-1 Peptidomimetics and the Development of a General-Purpose Model for Allosteric Modulators (ALLOPTML)

Ivo E. Sampaio-Dias,* José E. Rodríguez-Borges, Víctor Yáñez-Pérez, Sonia Arrasate, Javier Llorente, José M. Brea, Harbil Bediaga, Dolores Viña, María Isabel Loza, Olga Caamaño, Xerardo García-Mera,* and Humberto González-Díaz*

Cite This: https://dx.doi.org/10.1021/acschemneuro.0c00687 Read Online

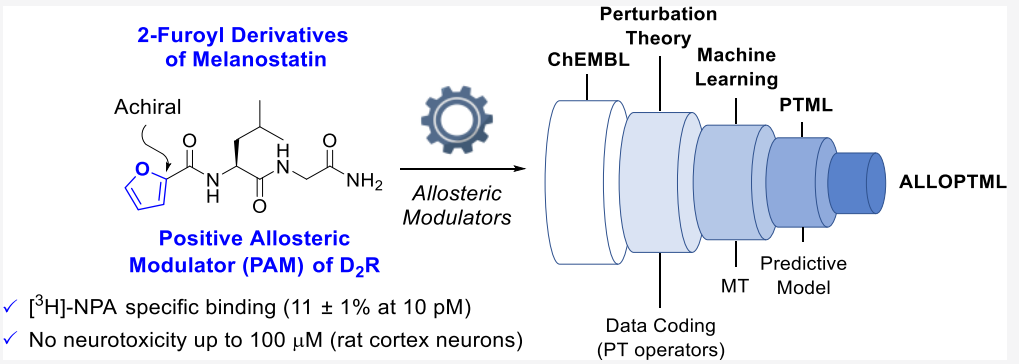

ABSTRACT: This work describes the synthesis and pharmacological evaluation of 2-furoyl-based Melanostatin (MIF-1) peptidomimetics as dopamine D_2 modulating agents. Eight novel peptidomimetics were tested for their ability to enhance the maximal effect of tritiated *N*-propylapomorphine ([^{3}H]-NPA) at D_2 receptors (D_2R). In this series, 2-furoyl-L-leucylglycinamide (**6a**) produced a statistically significant increase in the maximal [^{3}H]-NPA response at 10 pM (11 ± 1%), comparable to the effect of MIF-1 (18 ± 9%) at the same concentration. This result supports previous evidence that the replacement of proline residue by heteroaromatic scaffolds are tolerated at the allosteric binding site of MIF-1. Biological assays performed for peptidomimetic **6a** using cortex neurons from 19-day-old Wistar-Kyoto rat embryos suggest that **6a** displays no neurotoxicity up to 100 μM. Overall, the pharmacological and toxicological profile and the structural simplicity of **6a** makes this peptidomimetic a potential lead compound for further development and optimization, paving the way for the development of novel modulating agents of D_2R suitable for the treatment of CNS-related diseases. Additionally, the pharmacological and biological data herein reported, along with >20 000 outcomes of preclinical assays, was used to seek a general model to predict the allosteric modulatory potential of molecular candidates for a myriad of target receptors, organisms, cell lines, and biological activity parameters based on perturbation theory (PT) ideas and machine learning (ML) techniques, abbreviated as ALLOPTML. By doing so, ALLOPTML shows high specificity Sp = 89.2/89.4%, sensitivity Sn = 71.3/72.2%, and accuracy Ac = 86.1%/86.4% in training/validation series, respectively. To the best of our knowledge, ALLOPTML is the first general-purpose chemoinformatic tool using a PTML-based model for the multioutput and multicondition prediction of allosteric compounds, which is expected to save both time and resources during the early drug discovery of allosteric modulators.

KEYWORDS: *Allosteric modulators, artificial neural networks, big data, ChEMBL, machine learning, Melanostatin, multitarget models, perturbation theory*

1. INTRODUCTION

Dopamine receptors belong to a complex monoaminergic family of G protein-coupled receptors (GPCRs) represented by five distinct receptors (D_{1-5} receptors),[1] which are grouped into D_1-like (related to excitatory neurotransmission and composed by D_1 and D_5 isoforms) and D_2-like receptors (associated with inhibitory neurotransmission, comprising D_2, D_3, and D_4

Received: October 22, 2020
Accepted: December 7, 2020

isoforms).[1] These two subgroups differ in their signal transduction, binding profile, and physiological effects.[2] Among the D_{1-5} receptors, D_2-like receptors are considered of utmost importance due to their intrinsic role in the pathophysiology of neurological and psychiatric disorders.[3] Alternative splicing leads to generation of two distinct D_2 receptors (D_2Rs): D_2 short (D_{2S}) and D_2 long (D_{2L}) isoforms, which are associated with presynaptic and postsynaptic populations of D_2R, respectively.[4] The difference between these two splicing isoforms consist of 29 amino acid residues located in the III intracellular loop, responsible for the G protein coupling.[4] The design of ligands with receptor specificity is considered a herculean task due to the high structural homology shared by the members of D_1-like or D_2-like receptors.[3] For example, while D_2R is the main target to control the positive symptoms of schizophrenia, none of antipsychotics approved are capable to discriminate D_2 from D_3 receptors.[3] In this sense, allosteric regulation is considered a key pharmacological approach to selectively modulate the responsiveness of a specific receptor subtype with negligible or absent interference on the other subtypes. For this reason, allosteric modulators may contribute to the development of new selective and less toxic therapies than those focused on the orthosteric sites.[5] Allosteric modulators bind to a topological region of the receptor (i.e., an allosteric site) different from the binding site used by endogenous ligands (i.e., the orthosteric site). Upon binding, allosteric modulators induce structural modification that can either stabilize the active form of the receptor (positive modulation), inactivate it (negative modulation), or have no influence on the ligand−receptor binding (silent or neutral modulation).[6]

Positive allosteric modulators (PAMs) operate by either lowering the energy barrier necessary to achieve the active conformation of a given protein, by stabilizing its active conformation (preventing it from adopting nonactive conformations), or both.[7] PAMs do not display any activity or pharmacological effect in the absence of the endo/exogenous agonists, but when combined with an orthosteric agonist, they increase its efficacy, thus minimizing the overall side-effect profile of the agonist.[7]

An example of a PAM with intrinsic D_2 selectivity is the neuropeptide L-prolyl-L-leucylglycinamide,[8−12] also known as Melanostatin[8] or as melanocyte stimulating hormone release inhibiting factor 1 (MIF-1, Figure 1).[11]

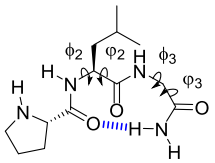

Figure 1. Melanostatin (MIF-1) structure denoting a type-II β-turn as the bioactive conformation assisted by an intramolecular hydrogen bond (dashed blue line).

MIF-1 is formed by exocyclic cleavage of oxytocin hormone and displays several biological activities within the central nervous system (CNS),[13] acting mainly as a neuronal modulating agent in the nigrostriatal pathway.[14] Pharmacologically, MIF-1 interacts with D_2R increasing the effect of dopaminergic agonists on these receptors such as *N*-propylnorapomorphine (NPA), apomorphine, and 2-amino-6,7-dihydroxy-3,4-tetrahydronaphthalene (ADTN).[8] Studies show that MIF-1 potentiates the binding of [^{3}H]-NPA and [^{3}H]-quinpirrole in a dose-dependent manner to D_{2L}, D_{2S}, and D_4 receptor subtypes to give a bell-shaped dose−response curve,[15] without enhancing the binding to D_1 and D_3 receptors.[8,14] Mechanistically, it is suggested that MIF-1 stabilizes D_2R into a high-affinity state, making this receptor more sensitive to agonists.[14,16,17] It is speculated that MIF-1 may have a direct interaction with a domain of the receptor other than its orthosteric site or that it may display an indirect mechanism associated with the increase of the rate of GTP hydrolysis promoted by G protein.[18] However, this last hypothesis seems less likely as the modulatory effect is not observed in other G protein-coupled receptors, such as α_2 adrenergic receptors, or with G_s-coupled receptors, such as D_1R family, thus showing D_2R specificity.[8]

Regarding its PAM activity and D_2R selectivity, MIF-1 has been proposed as an attractive drug candidate for further development in the treatment of CNS-related neurodegenerative diseases associated with dopamine receptor sensitivity, such as Parkinson's disease (PD), schizophrenia, tardive dyskinesia, and Gilles de la Tourette syndrome.[19] For example, MIF-1 is widely acknowledged for alleviating the behavioral changes in animal models of PD.[20,21] Furthermore, this neuropeptide also has the ability to interact with other drugs by modifying their effects[22] (e.g., MIF-1 antagonizes morphine-induced catalepsy as well as dyskinesia induced by antipsychotic drugs).[23−25] X-ray crystallography[26] and structure−activity relationship studies using constrained peptidomimetics[27] suggest that MIF-1 adopts a type-II β-turn formed by intramolecular hydrogen bonding between the carbonyl oxygen atom of the L-proline residue and the *trans* amide proton of the glycinamide residue (depicted as dashed blue line in Figure 1). The presence of the C-terminal carboxamide is considered a key pharmacophore for the modulatory activity of MIF-1 and its active peptidomimetics, however an extended bioactive conformation is also suggested.[16] Modifications in the proline residue of MIF-1 have long been recognized to render bioactive peptidomimetics,[28] indicating that this residue may be suitable for chemical derivatization and the development of novel bioactive PAMs.[10−12]

In this work, we aimed to explore 2-furoic acid (**2-Fu**) as proline surrogate for the assembly and pharmacological evaluation of a novel class of MIF-1 peptidomimetics as PAMs of D_2R. In addition, we intended to use the experimental data to construct a general-purpose computational model based on perturbation theory (PT) ideas and machine learning (ML) techniques to predict allosteric modulators for a myriad of receptor targets, organisms, cell lines, and biological activity parameters, abbreviated as ALLOPTML.

2. RESULTS AND DISCUSSION

Design and Chemistry. Proline has long been established as a nonessential amino acid residue for the activity of MIF-1 analogues,[28] thereby offering the possibility for the design of novel MIF-1 peptidomimetics with PAM activity and D_2 selectivity. For example, picolinic acid has been successfully used as proline surrogate for the assembly of MIF-1 analogues with PAM activity and suitable toxicological profile.[11] These findings led us to hypothesize that heterocyclic scaffolds may be tolerated at the putative allosteric binding site of D_2R. In this sense, to gain further insights into the architecture of D_2R allosteric pocket, the use of different heteroaromatic scaffolds may allow to further rationalize the chemical features required

https://dx.doi.org/10.1021/acschemneuro.0c00687
ACS Chem. Neurosci. XXXX, XXX, XXX−XXX

Scheme 1. Synthesis of 2-Furoyl-Based Peptidomimetics 4−7(a,b)[a]

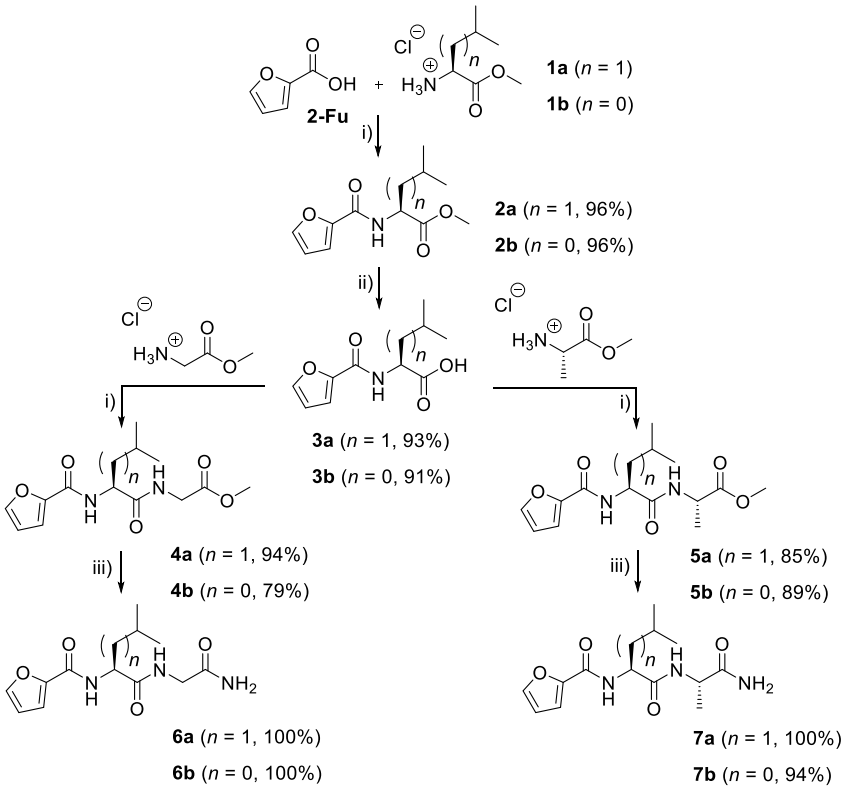

[a]Reagents and conditions: (i) DIEA, TBTU, CH_2Cl_2; (ii) LiOH, MeOH/H_2O followed by H_2SO_4 1 M; (iii) NH_3 (g), MeOH.

for the development of pharmacologically active PAMs. Considering that proline contains a pyrrolidine heterocycle, five-membered heteroaromatic rings such as furan scaffolds may represent suitable proline bioisosters for the design of MIF-1 peptidomimetics and thus providing useful information about the size and the nature of the hydrogen bonding at the D_2R allosteric binding site. To the best of our knowledge, the application of furan moieties for the development of MIF-1 derivatives have not yet been reported. In this sense, **2-Fu** was investigated for the assembly of a novel class of MIF-1 peptidomimetics.

For the preparation of 2-furoyl-based MIF-1 peptidomimetics, a diversity-oriented synthesis (DOS) strategy was employed to create a set of structure-related amino acid combinations at the central and C-terminal positions. For this purpose, L-leucine was replaced by L-valine, whereas glycine was substituted by L-alanine. The synthetic route for the preparation of 2-furoyl peptidomimetics is depicted in Scheme 1.

Starting from **2-Fu**, the preparation of amides **2(a,b)** was performed by peptide coupling with L-leucine and L-valine, respectively (Scheme 1). For that purpose, TBTU was used as the peptide coupling reagent in the presence of Hünig's base.[10,12,29] After chromatographic purification, compounds **2(a,b)** were obtained in high yields (96%).

Next, compounds **2(a,b)** were saponified using LiOH followed by acidic workup with 1 M H_2SO_4 to obtain the corresponding carboxylic acids **3(a,b)**. Because furan system is sensitive to low pH, at which may result in acid-catalyzed ring opening phenomena,[30] special attention was required during the acidic workup. Therefore, the pH was carefully adjusted to 4 to prevent the formation of side products. Both peptide products **3(a,b)** were isolated in very good yields (91−93%) with no detection of acyclic side products (TLC, NMR) under this protocol, as corroborated by the NMR data (^{1}H, ^{13}C{^{1}H}, and DEPT-135) shown in Figures S5−S8 of Supporting Information. Carboxylic acids **3(a,b)** were then coupled with either glycine (a) or L-alanine (b) methyl esters using the same peptide coupling protocol, delivering **4(a,b)**/**5(a,b)** in good to very good yields (79−94%).

Finally, pseudopeptides **4(a,b)**/**5(a,b)** were converted into the corresponding C-terminal carboxamides **6(a,b)**/**7(a,b)** upon treatment with gaseous ammonia in methanol, prepared *in situ* by reacting $Ca(OH)_2$ and NH_4Cl at 100 °C. The reactions proceeded cleanly, albeit it took about 48 h for completion (TLC, NMR). After the removal of the volatiles, C-terminal carboxamides **6(a,b)**/**7(a,b)** were obtained in practically quantitative yields (94−100%), without the need of chromatographic purifications. Following this synthetic route, 2-furoyl peptidomimetics were successfully prepared in high global yields (69−84%).

Pharmacology. Eight novel MIF-1 peptidomimetics were tested for their ability to potentiate the maximum binding of the radiolabeled agonist *N*-propylnorapomorphine, [^{3}H]-NPA, to cloned human dopamine D_{2S} receptors, and their activity was compared to that of MIF-1 as described in the literature.[8] Peptidomimetics **4−7(a,b)** were tested at eight different concentrations (between 1 pM and 10 μM) following the protocol previously reported in our research group.[10,12] The whole set of peptidomimetics was evaluated *in silico* to rule out the possibility of these ligands acting as promiscuous pan-assay interference compounds (PAINS) and/or aggregators.[31] The experimental results obtained for the binding assays are shown in Table 1 and Figure 2.

https://dx.doi.org/10.1021/acschemneuro.0c00687
ACS Chem. Neurosci. XXXX, XXX, XXX−XXX

Table 1. Experimental Results for MIF-1 Derivatives 4-7(a,b) in the D_2R Binding Assays

Cpnd	% [^{3}H]-NPA$_{max}$	AUC	Log (1/C_{max})
4a	11	53.72	10
4b	9	34.35	12
5a	11	27.25	10
5b	6	9.36	12
6a	11	12.98	11
6b	nd[a]	0	nd
7a	3	2.76	12
7b	nd	0	nd
MIF-1	22	44.19	10

[a]nd = not detected.

A statistically significant enhancement ($P < 0.05$; ANOVA test; post hoc Dunnet T3 test) of the [^{3}H]-NPA response was observed for peptidomimetic **6a** (Figure 2). The maximum specific binding of [^{3}H]-NPA elicited by **6a** was 11 ± 1% at 10 pM, while MIF-1 (positive control) displays [^{3}H]-NPA binding of 18 ± 9% at the same concentration and maximum effect of 22 ± 9% at 100 pM, as shown in Table 1 and Figure 2. In respect with the other peptidomimetics, no statistically significant increase in the [^{3}H]-NPA binding was observed, therefore no conclusion can be drawn for these compounds. In this work it was found that MIF-1 displays an increase in the [^{3}H]-NPA binding at lower concentrations than those previously reported by Verma and co-workers.[8] Because allosteric modulators are sensitive to environmental changes elicited by endogenous agonists on GPCRs,[32] this deviation may be attributed to the host cells used for expressing human D_{2S} receptors, which differ from the ones originally reported.[8]

The C-terminal carboxamide is widely recognized as a key pharmacophore for the activity of MIF-1 and its peptidomimetics,[33,9] which is crucial for these compounds to adopt the postulated type-II β-turn bioactive conformation.[33,9] However, Saitton and co-workers suggested the possibility for an extended bioactive conformation of MIF-1 through the development of bioactive peptidomimetics incorporating a 2,3,4-trisubstituted pyridine scaffold as leucyl mimetic preventing it from adopting the postulated type-II β-turn.[16] Like MIF-1, peptidomimetic **6a** displays the L-leucylglycinamide dipeptide motif; therefore, a type-II β-turn conformation is envisioned for this compound. Interestingly, the simple substitution of proline residue by **2-Fu** proved to effectively mimic the MIF-1 modulatory activity at D_2R allosteric binding site. The activity of **6a** is thus considered of utmost interest, because it endorses previous findings that achiral and heteroaromatic scaffolds are tolerated in the putative MIF-1 binding pocket, establishing proline as a key residue for derivatization in the development of MIF-1 analogues with PAM activity.

***In Vitro* Neurotoxicity Profile of 2-Furoyl MIF-1 Peptidomimetics.** Low nonspecific cytotoxicity is an important feature of lead compounds during early drug development. Therefore, peptidomimetics **4−7(a,b)** were evaluated to assess their neurotoxic profiles using culture of motor cortex neurons from 19-day-old Wistar-Kyoto (WKY) rat embryos.[11,34] Hydrogen peroxide, H_2O_2, was selected as a standard control for neurocytotoxity.[48,72,35] In fact, the majority of the *in vitro* neurotoxicity studies carried out in cortical

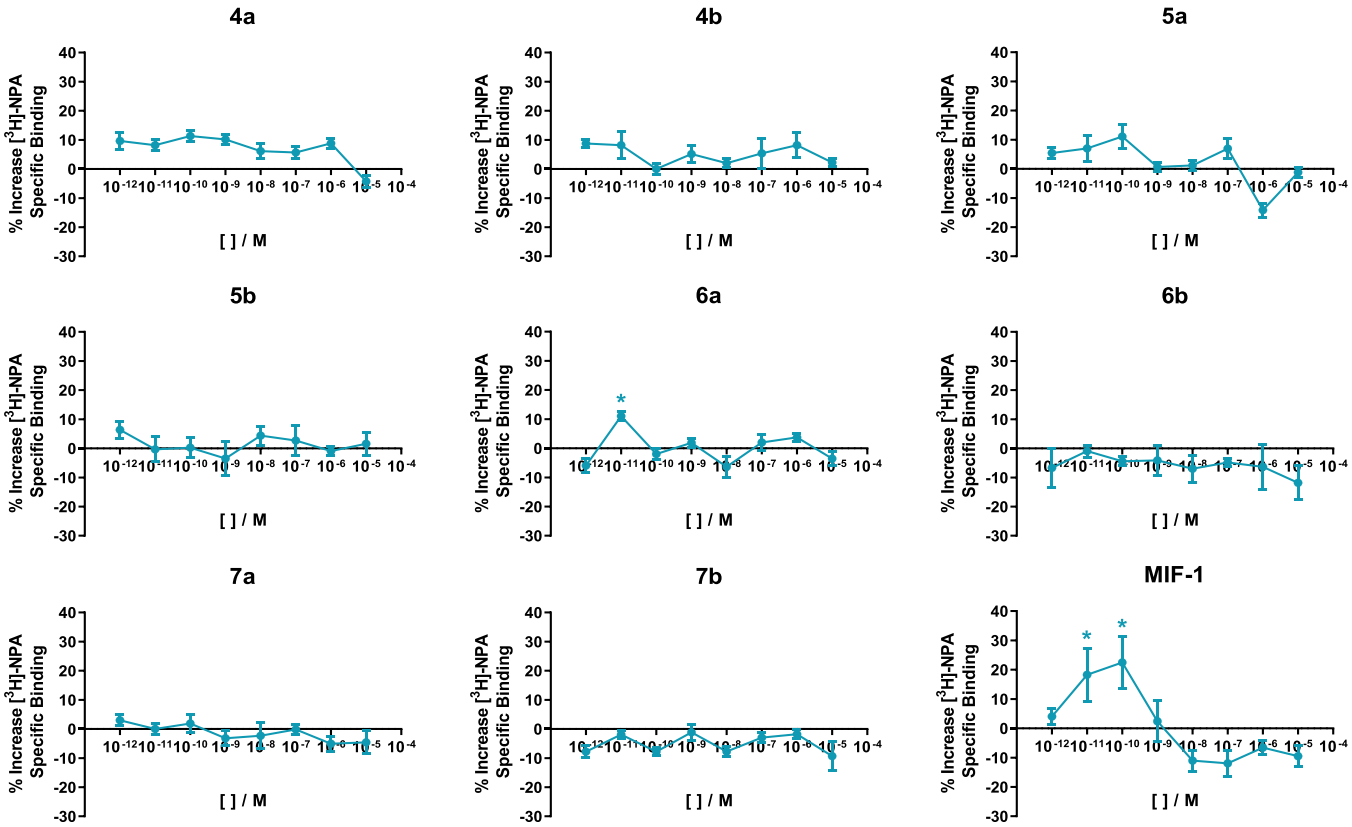

Figure 2. Modulation of the [^{3}H]-NPA binding by 2-furoyl-based MIF-1 peptidomimetics **4−7(a,b)** at eight different concentrations. Points represent the mean ± standard deviation (vertical bars) of three independent experiments carried out with duplicates. *$P < 0.05$ (ANOVA test; *posthoc* Dunnet T3 test).

https://dx.doi.org/10.1021/acschemneuro.0c00687
ACS Chem. Neurosci. XXXX, XXX, XXX−XXX

neurons uses H_2O_2 as an effective inducer of oxidative stress.[36] The use of H_2O_2 creates an imbalance between reactive oxygen species (ROS) levels and scavenging processes.[36] Excessive cell exposure to free radicals subsequently leads to neuronal death. In this assay, cellular viability was estimated based on the ability of cells to reduce MTT after a 24 h incubation period with the test compounds (100 μM). The percentage of cell viability was compared with the dimethyl sulfoxide (DMSO, negative control). All results are expressed as mean ± SEM of five independent experiments (Figure 3).

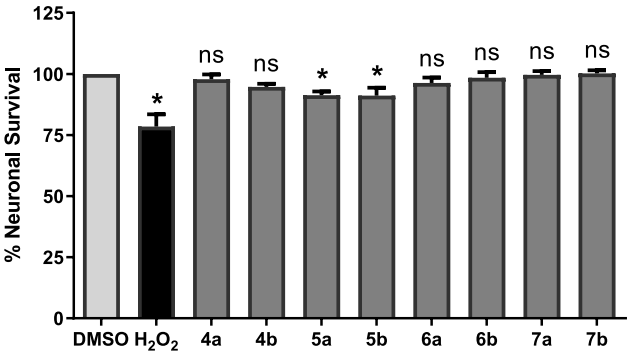

Figure 3. Neurotoxicity assays for peptidomimetics **4−7(a,b)** in cultured neurons from embryonic motor cortices of fetal Wistar-Kyoto rats. Data are the mean ± SEM of $n = 5$ independent experiments at 100 μM. Negative control = DMSO; positive control = 100 μM H_2O_2. *Level of statistical significance = $P < 0.05$ vs DMSO condition by t test.

As expected, the stress inducer (100 μM H_2O_2) reduced the cell survival to 78.51 ± 4.97% compared to the nontreated cells control ($P < 0.05$). In this assay compounds **5a** and **5b** display a statistically significant decrease in neuronal survival (91.34 ± 1.50 and 91.13 ± 3.20%, respectively, $P < 0.05$), in comparison with DMSO condition, suggesting these peptidomimetics exhibit a marginal neurotoxicity. The cell viability was not affected by the presence of the remaining test compounds when compared to the control (DMSO). These results indicate that 2-furoyl-based MIF-1 analogues display a safe profile up to 100 μM.

General-Purpose Model for Allosteric Modulators (ALLOPTML). The application and combination of computational methods and predictive software tools in medicinal chemistry are considered of utmost interest, enabling one to identify, prioritize, and optimize novel chemotypes with desired pharmacological activity profiles.[37] Computational models and algorithms capable to make predictions on the pharmacological and biological activity using different conditions of assay with minimal computational cost are thus highly desired. These powerful computer-aided models are useful to guide molecular design and decision making in drug discovery, boosting the identification of lead compounds avoiding time-consuming assays and saving resources; therefore, it is considered an essential pillar of modern drug research.[37]

In the absence of a robust and general-purpose model for the multioutput and multicondition prediction of allosteric compounds in medicinal chemistry, we sought to fill this gap. To achieve this goal, we developed and implemented ALLOPTML, abbreviation used to describe a novel predictive model for allosteric modulators based on perturbation theory (PT) ideas and machine learning (ML) techniques, which may be used for several types of systems and for a hundred different proteins. For this purpose, the pharmacological and biological data disclosed in this work for peptidomimetics **4−7(a,b)** was used to train the model along with the 21 439 cases from 8984 different ChEMBL assays of 8957 allosteric compounds for 79 different proteins. For this task 12 different variables ($\mathbf{c}_{0-11}$) were considered from the ChEMBL database big data (BD) sets of compounds covering 38 biological activity parameters ($\mathbf{c}_0$; e.g., efficacy, potency, intrinsic activity, IC_{50}, K_i, K_m), organisms of the protein target ($\mathbf{c}_1$; e.g., human, rat, mouse), organism of assay ($\mathbf{c}_2$; e.g., rat, swine, herpesvirus 5), different cellular lines ($\mathbf{c}_3$; e.g., CHO, HEK293), and so on. The general workflow used in this paper to obtain the PTML model is depicted in Figure 4.

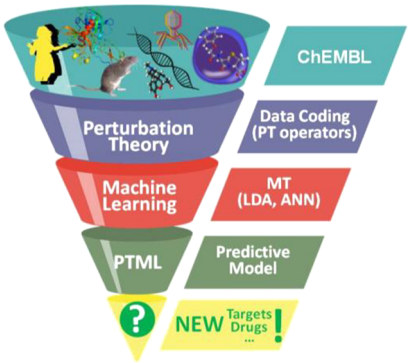

Figure 4. General workflow used to obtain the PTML model.

So far, finding allosteric binding sites and lead compounds has been largely serendipitous, accomplished by medicinal chemists through preclinical assays performing high-throughput screening with a high number of combinations of experimental conditions ($\mathbf{c}_{a,j}$). In addition, the existence of allo-network drugs, i.e., allosteric compounds that do not act directly over the pharmacological target but over a second protein which in turn interacts directly or indirectly with the target protein, makes this task even more challenging.[38−40] In addition to experimental techniques, computational techniques can be used to predict new drugs for different targets.[41] In this sense, many researchers have developed cheminformatics models for the discovery of new bioactive compounds. Nevertheless, almost all these models are designed for homologous series of compounds, one target, and/or a single cell line. Other models, instead, use heterogeneous series of compounds, although they are unable to incorporate information about the target, cell line, or organism of assay, among other features.[42−57] This drawback can be partially faced by ML techniques through which diverse molecular descriptors, encoding the chemical structure of different drugs, can be calculated.[58−74] ML techniques have already been carried out to predict allosteric pockets on proteins.[75] Unfortunately, this method failed to account for large BD sets of preclinical assays, such as the ChEMBL database, which are difficult to study due to the high complexity of the data in addition to the large volume of highly heterogeneous preclinical assays.[76,77]

To tackle this problem we have associated PT and ML modeling.[70,78] In fact, PTML (PT + ML) models have been used in many fields of knowledge such as medicinal chemistry, proteomics, or nanotechnology for modeling large data sets with BD features.[34,79−91] Probably due to the potential benefits of allosteric drugs, a renewed interest in allostery has led to the development of a number of computational approaches to understanding allostery.[92] Nevertheless, to the best of our

https://dx.doi.org/10.1021/acschemneuro.0c00687
ACS Chem. Neurosci. XXXX, XXX, XXX−XXX

Table 2. PTML Predictive Study of New Compounds

	c_0	EC_{50} (nM)	E_{max} (%)	% max	inhibition (%)
assay	c_1	*H. sapiens*	*H. sapiens*	*R. norvegicus*	*H. sapiens*
	c_2	*H. sapiens*	*H. sapiens*	*R. norvegicus*	*H. sapiens*
	c_3	HEK293	CHO	null	HEK293
	c_4	mGluR5[a]	mGluR2[a]	mGluR2	mGluR5
compound	**4a**	0.042	0.087	0.404	0.796
	4b	0.039	0.082	0.388	0.785
	5a	0.043	0.090	0.413	0.802
	5b	0.041	0.085	0.397	0.791
	6a	0.041	0.085	0.397	0.791
	6b	0.038	0.078	0.378	0.778
	7a	0.042	0.087	0.403	0.796
	7b	0.040	0.083	0.392	0.787
	MIF-1	0.036	0.076	0.368	0.770

[a]mGluR5 = metabotropic glutamate receptor 5 (CHEMBL2564 in rat and CHEMBL3227 in human); mGluR2 = metabotropic glutamate receptor 2 (CHEMBL5137 in human and CHEMBL2581 in rat).

knowledge, general-purpose PTML models for multiple preclinical assays of allosteric compounds have not yet been reported.

In training series, explored in detail in Supporting Information, the model presented high values of specificity, Sp = 89.2%; sensitivity, Sn = 71.3%; and accuracy, Ac = 86.1%. Likewise, the MMA model was also reliable in external validation series: Sp = 89.4%, Sn = 72.2%, and Ac = 86.4%. These values are in the range considered as useful for classification models with application in medicinal chemistry.[93]

Computational Study on the 2-Furoyl-Based MIF-1 Peptidomimetics. After training and validating the ALLOPTML model (Supporting Information), we decided to illustrate how to use it by providing a detailed step-by-step guide to calculate the posterior probabilities with a practical example. For this purpose, the series of peptidomimetics **4−7(a,b)** were studied in different assay conditions $\mathbf{c}_j$ (target proteins, cell lines, assay organisms). First, the chemical structures of peptidomimetics **4−7(a,b)** were drawn using ChemDraw software to obtain their SMILE codes. Then, the file containing all SMILE codes was created and uploaded to Virtual Computational Chemistry Laboratory (VCCLAB, http://www.vcclab.org, 2005)[94] in order to calculate the molecular descriptors D_k (Log *P*, PSA) for each compound. Because the goal was to illustrate how to operate the model, only a few assay conditions were selected. After that, the function of reference $f(\nu_{ij})_{ref}$ (expected probability of activity) values for each assay were obtained from Supporting Information. Using this file, the expected or average values $<D_k(\mathbf{c}_j)>$ of the molecular descriptors D_k were also obtained for all compounds assayed on these conditions. With these values in hand, we calculated the MMA operators $\Delta D_k(\mathbf{c}_j)$ for each compound vs every set of experimental conditions selected. Subsequently, $f(\nu_{ij})_{ref}$ and $\Delta D_k(\mathbf{c}_j)$ values were substituted into the equation of the model to obtain the values of the output function $f(\nu_{ij})_{calc}$. Lastly, these values were used to calculate the posterior probabilities $p(f(\nu_{ij})_{pred} = 1)$, with which the compounds may be considered as candidates for assay according to our criteria. The equation used to calculate these probabilities was a sigmoid function $p(f(\nu_{ij})_{pred} = 1) = 1/(1 + (\pi_0/\pi_1)\cdot \mathrm{Exp}(-f(\nu_{ij})_{calc})$. Recall that $\pi_1 = 1 - \pi_0$ are the probabilities (defined before to seek the model) with which a compound may be considered as active $f(\nu_{ij})_{pred} = 1$ or nonactive and $f(\nu_{ij})_{pred} = 0$, *a priori*.

In Table 2, the results obtained for the selected examples including different c_0 = activity parameter (units) such as effective 50% concentration EC_{50} (nM), maximun effect E_{max} (%), and inhibition (%) = inhibition (%) are listed. The examples also involve two different organisms (human and rat) expressing the protein target and organisms of assays (c_1 and c_2). We also changed the condition c_3 = cell line of assay (HEK293, CHO) and the condition c_4 = target proteins (mGluR5 and mGluR2). Interestingly, the model predicts a similar behavior for all the series of compounds in the same conditions, which is reasonably for a homogeneous series of compounds. The model predicts low probabilities of having interesting EC_{50} (nM) values for mGluR5 but high probabilities of inhibition (%) for the same receptor. This may be indicative that this set of peptidomimetics display activity on human mGluR5 but perhaps at higher concentrations.

3. CONCLUSIONS

The use of **2-Fu** for the assembly of MIF-1 peptidomimetics is unprecedented. In this work, a small library of MIF-1 peptidomimetics bearing **2-Fu** as proline surrogate was successfully obtained and pharmacologically evaluated toward D_2R. Remarkably, compound **6a** stands out as a D_2R modulator capable of increasing the maximal [^{3}H]-NPA response at 10 pM (11 ± 1%), comparable to the effect of MIF-1 (18 ± 9%) at the same concentration and with no neurotoxic effect up to 100 μM in cortex neurons of Wistar-Kyoto rat embryos. These findings corroborate that D_2R allosteric binding site can accommodate heteroaromatic rings at N-terminal position of MIF-1, establishing furan as a suitable heterocyclic scaffold to be used as proline mimetic for the assembly of MIF-1 analogues. Consequently, **6a** is considered a valid lead compound for further optimization, paving the way for the discovery of adequate candidates to treat CNS-related diseases. Exploration of other furan motifs is currently underway in our research group and will be disclosed in due time.

The topology of a complex network of allosteric modulators was constructed and studied delivering a predictive model, ALLOPTML, which shows remarkable specificity Sp = 89.2/89.4%, sensitivity Sn = 71.3/72.2%, and accuracy Ac = 86.1%/86.4% in training/validation series. The linear model with multicondition MAs proved to be superior to a linear model with simple condition MAs. To the best of our knowledge, ALLOPTML is the first general-purpose medicinal chemistry

https://dx.doi.org/10.1021/acschemneuro.0c00687
ACS Chem. Neurosci. XXXX, XXX, XXX−XXX

tool using PTML model for the multioutput and multicondition prediction of allosteric compounds, which is expected to be a valuable chemoinformatic tool to assist in the early drug discovery, saving both time and resources.

■ EXPERIMENTAL METHODS

Chemistry. All chemicals were of reagent grade and used without further purifications: 2-Furoic acid was obtained from Alfa Aesar; *O*-(Benzotriazol-1-yl)-*N,N,N′,N′*-tetramethyluronium tetrafluoroborate (TBTU), H-L-Leu-OMe, H-L-Val-OMe, H-L-Ala-OMe, and H-Gly-OMe were obtained from Bachem, and *N,N*-diisopropylethylamine (DIEA) was obtained from Sigma-Aldrich. All air sensitive reactions were carried out under argon atmosphere. Analytical TLC was carried out on precoated silica gel plates (Merck 60 F_{254}, 0.25 mm) using UV light and an ethanolic solution of phosphomolybdic acid (followed by gentle heating) for visualization. Flash chromatography was performed on silica gel (Merck 60, 230−240 mesh).

Apparatus. Mass spectra were recorded on a LTQ OrbitrapTM XL hybrid mass spectrometer (Thermo Fischer Scientific, Bremen, Germany) controlled by LTQ Tune Plus 2.5.5 and Xcalibur 2.1.0 (Centro de Materiais da Universidade do Porto, CEMUP). The capillary voltage of the electrospray ionization source (ESI) was set to 3.1 kV. The capillary temperature was set at 275 °C. The sheath gas was set at 6 (arbitrary unit as provided by the software settings). The capillary voltage was set at 35 V and the tube lens voltage set at 110 V. ^{1}H and ^{13}C NMR spectra were recorded at CEMUP with a Bruker Avance III 400 at 400.15 and 100.62 MHz, respectively. The ^{1}H NMR spectra were calibrated using the residual protic signals from the deuterated solvents while ^{13}C NMR spectra were calibrated directly from the deuterated solvents ($CDCl_3$: δ_H = 7.26, δ_C = 77.16; CD_3OD: δ_H = 3.31, δ_C = 49.00; and DMSO-d_6: δ_H = 2.50, δ_C = 39.52)[95] and are reported in parts per million (ppm). The nomenclature used for the assignment of protons and/or carbons for each α-amino acid residue in peptidomimetics was made using a single letter system in subscript for the amino acid residue (Leu = L-leucine; Val = L-valine, Ala = L-alanine; Gly = glycine) and indicating the proton (or group of protons) and/or the carbons in the structures by starting the numeration at the carbonyl carbon of the main chain of each α-amino acid residue. Optical rotations were measured on a JASCO P-2000 thermostated polarimeter using a sodium lamp and are reported as follows: α_D^θ expressed in (deg) (dm^{-1}) (g^{-1}), in which θ is the temperature in Celsius and c (g/100 mL, solvent). Melting points were determined using a STUART Scientific, model SMP1, and are not corrected. Solvents were evaporated in a Büchi rotavapor model R-210.

General Protocol for Peptide Coupling: Synthesis of 2(a,b), 4(a,b), and 5(a,b). The appropriate carboxylic acid (1 equiv) was charged in a round-bottom flask and dissolved in anhydrous CH_2Cl_2 (50 mL), under argon atmosphere, followed by iterative addition of DIEA (3 equiv) and TBTU (1.1 equiv), with stirring for 30 min at RT. Finally, the appropriate amine (1.2 equiv) was added, and the reaction was left stirring for approximately 1 h. After completion of the reaction (TLC), CH_2Cl_2 was removed *in vacuo*, and the crude oil was dissolved with EtOAc (100 mL) and transferred to a separatory funnel. The organic layer was washed with saturated solutions of $NaHCO_3$ (3 × 100 mL) and NaCl (100 mL) and dried over anhydrous Na_2SO_4. After filtration, the solvent was removed *in vacuo*, and the crude oil was chromatographed as specified for each peptide product.

General Protocol for Saponification: Synthesis of Pseudodipeptides 3(a,b). Pseudodipeptide methyl ester (1 equiv) was charged in a round-bottom flask, dissolved in MeOH (50 mL), and the solution was cooled at 0 °C using an ice bath with magnetic stirring. Then, LiOH (3 equiv) was slowly added during a period of 30 min and left stirring until complete consumption of the starting material (TLC). The solvent was removed *in vacuo* (at 40 °C), and the crude solid was then dissolved in water (20 mL), cooled at 0 °C using an ice bath with magnetic stirring. After that, 1 M H_2SO_4 was carefully added until pH = 4. The solvent was distilled off (at 40 °C), and the crude solid was then triturated with hot $CHCl_3$ and filtered. Removal of the volatiles were performed in a rotatory evaporator to afford the desired compound without further purifications.

General Protocol for C-Terminal Carboxamide: Synthesis of Pseudotripeptides 6(a,b) and 7(a,b). Pseudotripeptide methyl ester (1 equiv) was charged in a reaction flask and dissolved in MeOH p.a. (40 mL). The solution was cooled at 0 °C using an ice bath and gaseous ammonia (generated *in situ* by mixing NH_4Cl and $Ca(OH)_2$ 2:1 (w/w) at 100 °C using an oil bath) was bubbled into the reaction flask. The ammonia stream was maintained for 1 h, and the reaction was left stirring at room temperature (ca. 25 °C) until completion (ca. 48 h, TLC). Removal of the volatiles were performed in a rotatory evaporator to afford the desired compound without the need of chromatographic purification.

*Methyl 2-Furoyl-L-leucinate (**2a**).* Following the general protocol for peptide coupling, DIEA (4.66 mL, 26.8 mmol), TBTU (3.15 g, 9.81 mmol), and methyl L-leucinate hydrochloride (1.94 g, 10.7 mmol) was added to a solution of **2-Fu** (1.00 g, 8.92 mmol) in anhydrous CH_2Cl_2 (30 mL). After the typical workup, the crude oil was chromatographed using EtOAc as eluent, affording 2.05 g of **2a** as a white solid. Yield: 96%. m.p.: 83−87 °C. R_f: 0.84 in EtOAc. $[\alpha]_D^{24}$: +8.3 (c1, $CHCl_3$). ^{1}H NMR ($CDCl_3$, 400 MHz) δ ppm: 7.56−7.36 (m, 1H, H-5), 7.23−7.00 (m, 1H, H-3), 6.77 (d, J = 8.0 Hz, 1H, CONH), 6.59−6.38 (m, 1H, H-4), 4.82 (dt, J = 8.6, 4.9 Hz, 1H, H_{Leu}-2), 3.76 (s, 3H, CO_2CH_3), 1.89−1.52 (m, 3H, H_{Leu}-3 + H_{Leu}-4), 1.11−0.82 (m, 6H, H_{Leu}-5). ^{13}C NMR and DEPT ($CDCl_3$, 101 MHz) δ ppm: 173.4 (C, CO_2CH_3), 158.1 (C, CONH), 147.6 (C, C-2), 144.2 (CH, C-5), 114.8 (CH, C-3), 112.3 (CH, C-4), 52.4 (CH_3, CO_2CH_3), 50.4 (CH, C_{Leu}-2), 41.9 (CH_2, C_{Leu}-3), 25.0 (CH, C_{Leu}-4), 22.9 (CH_3, C_{Leu}-5), 22.0 (CH_3, C_{Leu}-5). HRMS (ESI-TOF) m/z: $[M + H]^+$ Calcd for $C_{12}H_{18}NO_4^+$, 240.123 03; found, 240.123 12.

*Methyl 2-Furoyl-L-Valinate (**2b**).* Following the general protocol for peptide coupling, DIEA (7.00 mL, 40.2 mmol), TBTU (4.7340 g, 14.743 mmol), and methyl L-valinate hydrochloride (2.6960 g, 16.084 mmol) was added to a solution of **2-Fu** (1.5022 g, 13.403 mmol) in anhydrous CH_2Cl_2 (30 mL). After the typical workup, the crude oil was chromatographed using EtOAc as eluent, affording 2.8981 g of **2b** as a white solid. Yield: 96%. m.p.: 75−78 °C. R_f: 0.89 in EtOAc. $[\alpha]_D^{21}$: +9.0 (c1.015, $CHCl_3$). ^{1}H NMR ($CDCl_3$, 400 MHz) δ ppm: 7.45 (dd, J = 1.8, 0.8 Hz, 1H, H-5), 7.10 (dd, J = 3.5, 0.8 Hz, 1H, H-3), 6.80 (d, J = 8.3 Hz, 1H, CONH), 6.48 (dd, J = 3.5, 1.8 Hz, 1H, H-4), 4.70 (dd, J = 9.0, 5.0 Hz, 1H, H_{Val}-2), 3.74 (s, 3H, CO_2CH_3), 2.24 (dhept, J = 6.9, 5.1 Hz, 1H, H_{Val}-3), [0.98 (d, J = 6.9 Hz, 3H), 0.95 (d, J = 6.9 Hz, 3H), H_{Val}-4]. ^{13}C NMR and DEPT ($CDCl_3$, 101 MHz) δ ppm: 172.4 (C, CO_2CH_3), 158.2 (C, CONH), 147.7 (C, C-2), 144.2 (CH, C-5), 114.8 (CH, C-3), 112.3 (CH, C-4), 56.8 (CH_3, CO_2CH_3), 52.3 (CH, C_{Val}-2), 31.6 (CH, C_{Val}-3), 19.1 (CH, C_{Val}-4), 17.9 (CH, C_{Val}-4). HRMS (ESI-TOF) m/z: $[M + H]^+$ Calcd for $C_{11}H_{16}NO_4^+$, 226.107 38; found, 226.107 38.

*2-Furoyl-L-leucine (**3a**).* Following the general protocol for saponification, LiOH (0.2414 g, 10.08 mmol) was added to a solution of **2a** (0.8034 g, 3.360 mmol) in MeOH (30 mL). After the typical workup, 0.7038 g of **3a** was obtained as a white solid. Yield: 93%. m.p.: 81−84 °C. R_f: 0.09 in EtOAc. $[\alpha]_D^{24}$: +8.3 (c1, $CHCl_3$). ^{1}H NMR ($CDCl_3$, 400 MHz) δ ppm: 8.95 (br s, 1H, CO_2H), 7.41 (d, J = 1.3 Hz, 1H, H-5), 7.10 (d, J = 3.4 Hz, 1H, H-3), 7.06 (d, J = 7.9 Hz, 1H, CONH), 6.42 (dd, J = 3.4, 1.7 Hz, 1H, H-4), 4.76−4.61 (m, 1H, H_{Leu}-2), 1.80−1.57 (m, 3H, H_{Leu}-3 + H_{Leu}-4), 1.10−0.80 (m, 6H, H_{Leu}-5). ^{13}C NMR and DEPT ($CDCl_3$, 101 MHz) δ ppm: 177.6 (C, CO_2H), 158.7 (C, CONH), 147.3 (C, C-2), 144.6 (CH, C-5), 115.3 (CH, C-3), 112.3 (CH, C-4), 51.6 (CH, C_{Leu}-2), 41.5 (CH_2, C_{Leu}-3), 25.0 (CH, C_{Leu}-4), 23.1 (CH_3, C_{Leu}-5), 21.8 (CH_3, C_{Leu}-5). HRMS (ESI-TOF) m/z: $[M - H]^-$ Calcd for $C_{11}H_{14}NO_4^-$, 224.092 83; found, 224.094 82.

*2-Furoyl-L-valine (**3b**).* Following the general protocol for saponification, LiOH (0.2558 g, 10.68 mmol) was added to a solution of **2b** (0.8019, 3.560 mmol) in MeOH (30 mL). After the typical workup, 0.6843 g of **3b** was obtained as a white solid. Yield: 91%. m.p.: 65−70 °C. R_f: 0.05 in EtOAc. $[\alpha]_D^{20}$: +67.5 (c1.09, $CHCl_3$). ^{1}H NMR ($CDCl_3$, 400 MHz) δ ppm: 10.12 (br s, 1H, CO_2H), 7.42 (d, J = 0.9 Hz, 1H, H-5), 7.10 (d, J = 3.3 Hz, 1H, H-3), 7.04 (d, J = 8.5 Hz, 1H, CONH), 6.42 (dd, J = 3.4, 1.7 Hz, 1H, H-4), 4.60 (dd, J = 8.5, 5.1 Hz, 1H, H_{Val}-2), 2.37−2.13 (m, 1H, H_{Val}-3), 0.95 (d, J = 7.1 Hz, 3H, H_{Val}-

https://dx.doi.org/10.1021/acschemneuro.0c00687
ACS Chem. Neurosci. XXXX, XXX, XXX−XXX

4), 0.93 (d, J = 7.1 Hz, 3H, H_{Val}-4). ^{13}C NMR and DEPT ($CDCl_3$, 101 MHz) δ ppm: 176.2 (C, CO_2H), 158.8 (C, CONH), 147.3 (C, C-2), 144.6 (CH, C-5), 115.3 (CH, C-3), 112.3 (CH, C-4), 57.9 (CH, C_{Val}-2), 31.3 (CH, C_{Val}-3), 19.3 (CH, C_{Val}-4), 17.9 (CH, C_{Val}-4). HRMS (ESI-TOF) m/z: $[M - H]^-$ Calcd for $C_{10}H_{12}NO_4^-$, 210.077 18; found, 210.077 77.

*Methyl 2-Furoyl-L-leucylglycinate (**4a**).* Following the general protocol for peptide coupling, DIEA (2.06 mL, 11.8 mmol), TBTU (1.3933 g, 4.3393 mmol), and methyl glycinate hydrochloride (0.5942 g, 4.733 mmol) were added to a solution of **3a** (0.8767 g, 3.944 mmol) in anhydrous CH_2Cl_2 (30 mL). After the typical workup, the crude oil was chromatographed using EtOAc as eluent, affording 1.1394 g of **4a** as a white solid. Yield: 94%. m.p.: 135−136 °C. R_f: 0.58 in EtOAc. $[\alpha]_D^{20}$: −8.5 (c1, $CHCl_3$). ^{1}H NMR ($CDCl_3$, 400 MHz) δ ppm: 7.44−7.40 (m, 1H, H-5), 7.26−7.12 (m, 1H, CONH), 7.12−7.06 (m, 1H, H-3), 7.04−6.86 (m, 1H, CONH), 6.46 (dt, J = 4.8, 1.7 Hz, 1H, H-4), 4.82−4.64 (m, 1H, H_{Leu}-2), 4.13−3.87 (m, 2H, H_{Gly}-2), 3.76−3.63 [3.70 (s), 3.69 (s), 3H, CO_2CH_3], 1.87−1.53 (m, 3H, H_{Leu}-3 + H_{Leu}-4), 1.04−0.79 (m, 6H, H_{Leu}-5). ^{13}C NMR e DEPT ($CDCl_3$, 101 MHz) δ ppm: [172.5 (C), 172.4 (C), 170.2 (C), CONH + CO_2CH_3], 158.5 (C, CONH), 147.4 (C, C-2), 144.5 (CH, C-5), 115.0 (CH, C-3), 112.3 (CH, C-4), 52.4 (CH_3, CO_2CH_3), 51.3 (CH, C_{Leu}-2), 41.3 (2 CH_2, C_{Gly}-2 + C_{Leu}-3), 24.8 (CH, C_{Leu}-4), 23.0 (CH_3, C_{Leu}-5), 22.1 (CH_3, C_{Leu}-5). HRMS (ESI-TOF) m/z: $[M + H]^+$ Calcd for $C_{14}H_{21}N_2O_5^+$, 297.144 50; found, 297.143 77.

*Methyl 2-Furoyl-L-valylglycinate (**4b**).* Following the general protocol for peptide coupling, DIEA (3.70 mL, 21.3 mmol), TBTU (2.5089 g, 7.8138 mmol), and methyl glycinate hydrochloride (1.0701 g, 8.5242 mmol) were added to a solution of **3b** (1.5004 g, 7.1035 mmol) in anhydrous CH_2Cl_2 (30 mL). After the typical workup, the crude oil was chromatographed using EtOAc as eluent, affording 1.5842 g of **4b** as a white solid. Yield: 79%. m.p.: 133−136 °C. R_f: 0.60 in EtOAc. $[\alpha]_D^{22}$: −38.4 (c1.015, $CHCl_3$). ^{1}H NMR ($CDCl_3$, 400 MHz) δ ppm: 7.50−7.40 (m, 1H, H-5), 7.32 (br s, 1H, CONH), 7.20−7.00 [7.11 (dd, J = 6.9, 4.2 Hz), 7.09 (br s), H-3 + CONH], 6.49 (dd, J = 3.4, 1.7 Hz, 1H, H-4), 4.63−4.53 (m, 1H, H_{Val}-2), 4.20−3.90 (m, 2H, H_{Gly}-2), 3.73 (s, 3H, CO_2CH_3), 2.28−2.15 (m, 1H, H_{Val}-3), 1.12−0.92 (m, 6H, H_{Val}-4). ^{13}C NMR and DEPT ($CDCl_3$, 101 MHz) δ ppm: [171.6 (C), 170.2, CO_2CH_3 + CONH], 158.5 (C, CONH), 147.5 (C, C-2), 144.5 (CH, C-5), 114.8 (CH, C-3), 112.2 (CH, C-4), 58.1 (CH, C_{Val}-2), 52.4 (CH_3, CO_2CH_3), 41.2 (CH_2, C_{Gly}-2), 31.5 (CH, C_{Val}-3), 19.3 (CH, C_{Val}-4), 18.3 (CH, C_{Val}-4). HRMS (ESI-TOF) m/z: $[M + H]^+$ Calcd for $C_{13}H_{19}N_2O_5^+$, 283.128 85; found, 283.128 78.

*Methyl 2-Furoyl-L-leucyl-L-alaninate (**5a**).* Following the general protocol for peptide coupling, DIEA (3.92 mL, 22.5 mmol), TBTU (2.6506 g, 8.2550 mmol), and methyl L-alaninate hydrochloride (1.2570 g, 9.0054 mmol) were added to a solution of **3a** (1.6678 g, 7.5045 mmol) in anhydrous CH_2Cl_2 (30 mL). After the typical workup, the crude oil was chromatographed using EtOAc as eluent, affording 1.9797 g of **5a** as a white solid. Yield: 85%. m.p.: 135−136 °C. R_f: 0.58 in EtOAc. $[\alpha]_D^{22}$: +83.7 (c1.16, $CHCl_3$). ^{1}H NMR ($CDCl_3$, 400 MHz) δ ppm (rotamers present 60:40): [7.43 (dd, J = 1.7, 0.8 Hz, minor), 7.41 (dd, J = 1.7, 0.8 Hz, major), 1H, H-5], [7.11 (dd, J = 3.5, 0.7 Hz, minor), 7.09 (dd, J = 3.5, 0.7 Hz, major), 7.07 (br s), 2H, H-3 + CONH], [6.95 (d, J = 8.6 Hz, major), 6.91 (d, J = 8.6 Hz, minor), 1H, CONH], 6.51−6.41 (m, 1H, H-4), 4.78−4.66 (m, 1H, H_{Leu}-2), 4.60−4.47 (m, 1H, H_{Ala}-2), [3.72 (s, major), 3.66 (s, minor), 3H, CO_2CH_3], 1.78−1.59 (m, 3H, H_{Leu}-3 + H_{Leu}-4), [1.40 (d, J = 7.2 Hz, minor), 1.36 (d, J = 7.2 Hz, major), 3H, H_{Ala}-3], 0.94−0.90 (m, 6H, H_{Leu}-5). ^{13}C NMR and DEPT ($CDCl_3$, 101 MHz) δ ppm: [173.3 (C), 173.1 (C), 171.8 (C), 171.6 (C), CONH + CO_2CH_3], [158.4 (C), 158.3 (C), CONH], [147.6 (C), 147.5 (C), C-2], 144.4 (CH, C-5), [114.9 (CH), 114.8 (CH), C-3], [112.3 (CH), 112.2 (CH), C-4], 52.5 (CH_3, CO_2CH_3), [51.3 (CH), 51.2 (CH), C_{Leu}-2], [48.2 (CH), 48.2 (CH), C_{Ala}-2], [41.7 (CH_2), 41.5 (CH_2), C_{Leu}-3], [24.9 (CH), 24.8 (CH), C_{Leu}-4], [23.0 (CH_3), 23.0 (CH_3), C_{Ala}-3], [22.2 (CH_3), 22.2 (CH_3), 18.2 (CH_3), 18.0 (CH_3), C_{Leu}-5]. HRMS (ESI-TOF) m/z: $[M + H]^+$ Calcd for $C_{15}H_{23}N_2O_5^+$, 311.160 15; found, 311.158 26.

*Methyl 2-Furoyl-L-valyl-L-alaninate (**5b**).* Following the general protocol for peptide coupling, DIEA (1.24 mL, 7.12 mmol), TBTU (0.8381 g, 2.610 mmol), and methyl L-alaninate hydrochloride (0.3975 g, 2.848 mmol) were added to a solution of **3b** (0.5012 g, 2.373 mmol) in anhydrous CH_2Cl_2 (30 mL). After the typical workup, the crude oil was chromatographed using EtOAc as eluent, affording 0.6258 g of **5b** as a white solid. Yield: 89%. m.p.: 130−132 °C. R_f: 0.69 in EtOAc. $[\alpha]_D^{20}$: −8.1 (c1.01, DMSO). ^{1}H NMR ($CDCl_3$, 400 MHz) δ ppm (rotamers present 60:40): 7.44−7.40 (m, 1H, H-5), 7.40−7.26 [7.38 (d, J = 6.6 Hz, major), 7.29 (d, J = 6.9 Hz, minor), 1H, CONH], 7.19−6.99 [7.13 (d, J = 9.0 Hz), H-3 + CONH], 6.50−6.39 (m, 1H, H-4), 4.68−4.46 (m, 2H, H_{Val}-2 + H_{Ala}-2), [3.71 (s, major), 3.65 (s, minor), 3H, CO_2CH_3], 2.26−2.04 (m, 1H, H_{Val}-3), [1.40 (d, J = 7.2 Hz, minor), 1.36 (d, J = 7.3 Hz, major), 3H, H_{Ala}-3], 1.04−0.90 (m, 6H, H_{Val}-4). ^{13}C NMR and DEPT ($CDCl_3$, 101 MHz) δ ppm (rotamers present): [173.3 (C), 173.0 (C), 170.9 (C), 170.7 (C), CO_2CH_3 + CONH], [158.3 (C), 158.3 (C), CONH], [147.6 (C), 147.6 (C), C-2], [144.4 (CH), 144.4 (CH), C-5], [114.7 (CH), 114.7 (CH), C-3], [112.2 CH), 112.2 (CH), C-4], [57.8 (CH), 57.8 (CH), C_{Val}-2], [52.4 (CH_3), 52.4 (CH_3), CO_2CH_3], [48.2 (CH), 48.1 (CH), C_{Ala}-2], [31.9 (CH), 31.7 (CH), C_{Val}-3], [19.3 (CH_3), 19.1 (CH_3), 18.3 (CH_3), 18.2 (CH_3), 18.1 (CH_3), 17.8 (CH_3), C_{Val}-4 + C_{Ala}-3]. HRMS (ESI-TOF) m/z: $[M + H]^+$ Calcd for $C_{14}H_{21}N_2O_5^+$, 297.144 50; found, 297.144 63.

*Methyl 2-Furoyl-L-leucylglycinamide (**6a**).* Following the general protocol for the synthesis of primary amide, gaseous ammonia was bubbled into a solution of **4a** (0.3090 g, 1.043 mmol) in MeOH p.a. (20 mL), and the system was left stirring for 48 h at rt. After the typical workup, 0.2921 g of **6a** was obtained as a beige solid. Yield: quantitative. m.p.: 90−95 °C. R_f: 0.05 in EtOAc. $[\alpha]_D^{20}$: +161.2 (c1, $CHCl_3$). ^{1}H NMR ($CDCl_3$, 400 MHz) δ ppm: 8.01−7.77 (m, 1H, CONH), 7.49−7.32 (m, 2H, H-5 + CONH), 7.12−7.03 (m, 1H, H-3), 6.94 (br s, 1H, $CONH_2$), 6.48 (br s, 1H, $CONH_2$), 6.42 (dd, J = 3.1, 1.5 Hz, 1H, H-4), 4.74−4.50 (m, 1H, H_{Leu}-2), 3.98 (dd, J = 16.9, 6.1 Hz, 1H, H_{Gly}-2), 3.87−3.66 (m, 1H, H_{Gly}-2), 1.80−1.58 (m, 3H, H_{Leu}-3 + H_{Leu}-4), 0.99−0.81 (m, 6H, H_{Leu}-5). ^{13}C NMR and DEPT ($CDCl_3$, 101 MHz) δ ppm: [173.3 (C), 173.3 (C), 172.5 (C), 159.1 (C), 2 × CONH + $CONH_2$], 147.2 (C, C-2), 144.9 (CH, C-5), 115.1 (CH, C-3), 112.3 (CH, C-4), 52.3 (CH, C_{Leu}-2), 42.9 (CH_2, C_{Leu}-3), 41.0 (CH_2, C_{Gly}-2), 24.9 (CH, C_{Leu}-4), 23.0 (CH_3, C_{Leu}-5), 21.9 (CH_3, C_{Leu}-5). HRMS (ESI-TOF) m/z: $[M + H]^+$ Calcd for $C_{13}H_{20}N_3O_4^+$, 282.144 83; found, 282.144 17.

*Methyl 2-Furoyl-L-valylglycinamide (**6b**).* Following the general protocol for the synthesis of primary amide, gaseous ammonia was bubbled into a solution of **4b** (0.3819 g, 1.353 mmol) in MeOH p.a. (20 mL), and the system was left stirring for 48 h at rt. After the typical workup, 0.3611 g of **6b** was obtained as a white solid. Yield: quantitative. m.p.: 180−183 °C. R_f: 0.20 in EtOAc. $[\alpha]_D^{21}$: +14.6 (c1.025, DMSO). ^{1}H NMR (DMSO-d_6, 400 MHz) δ ppm: 8.30 (t, J = 5.8 Hz, 1H, CONH), 8.04 (d, J = 8.4 Hz, 1H, CONH), 7.87−7.82 (m, 1H, H-5), 7.29−7.15 [7.23 (br s), 7.21 (d, J = 3.5 Hz), 2H, CON*H*H + H-3], 7.04 (br s, 1H, CONH*H*), 6.63 (dd, J = 3.5, 1.8 Hz, 1H, H-4), 4.25 (dd, J = 8.1, 7.7 Hz, 1H, H_{Val}-2), [3.66 (dd, J = 16.7, 6.0 Hz), 3.65 (dd, J = 16.7, 5.5 Hz), 2H, H_{Gly}-2], 2.18−2.04 (m, 1H, H_{Val}-3), [0.91 (d, J = 6.8 Hz), 0.90 (d, J = 6.7 Hz), 6H, H_{Val}-4]. ^{13}C NMR and DEPT (DMSO-d_6, 101 MHz) δ ppm: [171.1 (C), 170.7 (C), 157.8 (C), 2 × CONH + $CONH_2$], 147.4 (C, C-2), 145.2 (CH, C-5), 114.0 (CH, C-3), 111.9 (CH, C-4), 58.3 (CH, C_{Val}-2), 41.8 (CH_2, C_{Gly}-2), 30.1 (CH, C_{Val}-3), [19.3 (CH_3), 18.6 (CH_3), C_{Val}-4]. HRMS (ESI-TOF) m/z: $[M + H]^+$ Calcd for $C_{12}H_{18}N_3O_4^+$, 268.129 18; found, 268.128 84.

*Methyl 2-Furoyl-L-leucyl-L-alaninamide (**7a**).* Following the general protocol for the synthesis of primary amide, gaseous ammonia was bubbled into a solution of **5a** (0.5552 g, 1.788 mmol) in MeOH p.a. (20 mL), and the system was left stirring for 48 h at rt. After the typical workup, 0.5279 g of **7a** was obtained as a white solid. Yield: quantitative. m.p.: 85−90 °C. R_f: 0.27 in EtOAc. $[\alpha]_D^{23}$: −36.6 (c1.015, $CHCl_3$). ^{1}H NMR ($CDCl_3$, 400 MHz) δ ppm (rotamers present 70:30): [7.84 (d, J = 7.8 Hz, minor), 7.76 (d, J = 7.5 Hz, major), 1H, CONH], 7.47−7.20 [7.44 (dd, J = 1.7, 0.7 Hz), 2H, H-5 + CONH], [7.13 (dd, J = 3.5, 0.6 Hz, major), 7.10 (dd, J = 3.6, 0.6 Hz, minor), 1H, H-3], [7.02 (br s, minor), 6.94 (br s, major), 1H, CON<u>H</u>H], 6.63−6.19 [6.42 (br s, minor), 6.38 (br s, major), 2H, H-4 + CONH<u>H</u>], 4.81−4.63 (m, 1H, H_{Leu}-2), [4.53 (p, J = 7.0 Hz), 4.52 (p, J = 7.1 Hz), 1H, H_{Ala}-2], 1.76−1.63 (m, 3H, H_{Leu}-3 + H_{Leu}-4), [1.39 (d, J = 7.1 Hz, minor), 1.33 (d, J =

https://dx.doi.org/10.1021/acschemneuro.0c00687
ACS Chem. Neurosci. XXXX, XXX, XXX−XXX

7.1 Hz, major), 3H, H_{Ala}-3], 0.98−0.87 (m, 6H, H_{Leu}-5). ^{13}C NMR and DEPT ($CDCl_3$, 101 MHz) δ ppm (rotamers present): [176.3 (C), 176.2 (C), 173.4 (C), 173.2 (C), 159.8 (C), 159.5 (C), 2 × CONH + $CONH_2$], [148.2 (C), 148.0 (C), C-2], [145.5 (CH), 145.4 (CH), C-5], [115.9 (CH), 115.8 (CH), C-3], 113.1 (CH, C-4), [53.0 (CH), 52.6 (CH), C_{Leu}-2], [49.7 (CH), 49.6 (CH), C_{Ala}-2], [42.3 (CH_2), 42.1 (CH_2), C_{Leu}-3], [25.7 (CH), 25.7 (CH), C_{Leu}-4], [23.8 (CH_3), 23.7 (CH_3), 22.9 (CH_3), 22.8 (CH_3), C_{Leu}-5], [18.8 (CH_3), 18.7 (CH_3), C_{Ala}-3]. HRMS (ESI-TOF) m/z: $[M + H]^+$ Calcd for $C_{14}H_{22}N_3O_4^+$, 296.160 48; found, 296.160 33.

*Methyl 2-Furoyl-L-valyl-L-alaninamide (**7b**).* Following the general protocol for the synthesis of primary amide, gaseous ammonia was bubbled into a solution of **5b** (0.4012 g, 1.353 mmol) in MeOH p.a. (20 mL), and the system was left stirring for 48 h at rt. After the typical workup, 0.3580 g of **7b** was obtained as a white solid. Yield: 94%. m.p.: 202−204 °C. R_f: 0.14 in Et_2O. $[\alpha]_D^{21}$: +4.3 (c1.04, DMSO). ^{1}H NMR (CD_3OD, 400 MHz) δ ppm (rotamers present 60:40): 7.75−7.58 (m, 1H, H-5), 7.25−7.07 (m, 1H, H-3), 6.66−6.50 [6.59 (dd, J = 3.5, 1.8 Hz), 6.58 (dd, J = 3.5, 1.8 Hz), 1H, H-4], 4.46−4.16 (m, 2H, H_{Val}-2 + H_{Ala}-2), 2.25−2.10 (m, 1H, H_{Val}-3), 1.42−1.33 [m, 3H, H_{Ala}-3], 1.08−0.93 (m, 6H, H_{Val}-4). ^{13}C NMR and DEPT, (CD_3OD, 101 MHz) δ ppm (rotamers present): [177.6 (C), 177.3 (C), 173.6 (C), 173.1 (C), 160.9 (C), 160.6 (C), 2 × CONH + $CONH_2$], [148.5 (C), 148.5 (C), C-2], 146.7 (CH, C-5), [115.9 (CH), 115.9 (CH), C-3], [113.1 CH), 113.0 (CH), C-4], [60.8 (CH), 59.9 (CH), C_{Val}-2], [50.1 (CH), 50.0 (CH), C_{Ala}-2], [32.2 (CH), 31.6 (CH), C_{Val}-3], [19.8 (CH_3), 19.6 (CH_3), 19.3 (CH_3), 18.9 (CH_3), 18.3 (CH_3), 18.0 (CH_3), C_{Val}-4 + C_{Ala}-3]. HRMS (ESI-TOF) m/z: $[M + H]^+$ Calcd for $C_{13}H_{20}N_3O_4^+$, 282.144 83; found, 282.144 37.

PHARMACOLOGY

Dopamine D_2 Receptor Binding Assay. Chinese hamster ovary (CHO) cells expressing short isoform of human D_{2S} receptors were grown in 150 mm Petri dishes in Dulbeco's Modified Eagle Medium (DMEM) supplemented with 10% FBS and 2 mM L-Glutamine. When cells were confluent, medium was removed, and cells were washed twice with buffer A (5 mM Tris−HCl pH = 7.4, 2 mM EDTA). Cells were scrapped and homogenized twice in a Polytron. Cell suspension was centrifuged (300 g, 10 min, 4 °C). Pellet was discarded, and supernatant was centrifuged (48 400 g; 4 °C; 60 min). Pellet was resuspended in buffer B (50 mM Tris−HCl; pH = 7.4), and protein quantity was measured by using Bradford method. The binding of [^{3}H]-NPA to the membrane preparation was assayed in duplicate in 96-well plates. Membranes (30 μg/well) expressing human D_2R were incubated with 0.25 nM [^{3}H]-NPA and test compounds for 60 min at 25 °C in a 96-well polypropylene microplate with incubation buffer (50 mM Tris−HCl, pH = 7.4; 120 mM NaCl, 5 mM KCl, 4 mM $MgCl_2$, 1 mM EDTA) up to a total volume of 250 μL. Nonspecific binding was defined in the presence of 1 μM (+)-butaclamol. After incubation time, 200 μL was transferred to a multiscreen FC microplate (Millipore) pretreated with 0.5% polyethilenimine, and samples were filtered and washed four times with 250 μL of wash buffer (50 mM Tris−HCl, pH = 7.4; 0.9% NaCl). Filters were dried, and 35 μL of scintillation cocktail (Universol) was added to each well; radioactivity was detected in a microplate beta scintillation counter (Microbeta Trilux). Data are expressed as the increase of specific binding following the formula:

$$\%\ \text{increase} = \frac{(X - \text{NSB}) \times 100}{\text{BT} - \text{NSB}} - 100$$

where X is the radioactivity detected in the test well, BT is the radioactivity detected when [^{3}H]-NPA was incubated in the absence of any compound, and NSB is the radioactivity detected when [^{3}H]-NPA was coincubated with 10 μM (+)-butaclamol. ANOVA analysis was carried out to evaluate significant differences using SPSS software (V15.0). Statistical significance was set at $P < 0.05$.

Biological Assays. *Animals.* Five female Wistar-Kyoto (WKY) rats (Iffa-Credo, L'Arbresele, Lyon, France), purchased from Criffa (Barcelona, Spain), were used throughout this study. They were housed (groups of five) in Makrolon cages (Panlab, Barcelona, Spain) on poplar shaving bedding (B&K Universal; G. Jordi, Barcelona, Spain) in a standard experimental animal Bioclean room, illuminated from 8:00 AM to 8:00 PM (12 h/12 h/light/dark cycle) and maintained at a temperature of 22 to 24 °C. Animals had free access to food pellets (B&K Universal) and drinking fluid (tap water). All animal experiments performed were conducted in compliance with institutional guidelines and European regulations on the protection of animals (Directive 2010/63/UE), the Spanish Real Decreto 53/2013 (1 February), and the Guide for the Care and Use of Laboratory Animals as adopted and promulgated by the US.

Culture of Rat Cortical Neurons and Glial Cells. Pregnant rats (19−20 days) were killed by CO_2 inhalation. Embryos were immediately extracted from the womb by caesarean section, and their brains were carefully dissected out. Meninges were removed, and a portion of motor cortex was isolated after the dissection of the brain. Fragments obtained from several embryos were subjected to mechanic disintegration. Neurobasal medium supplemented with 2% B-27 was used to seed the cells in 48-well plates at a density of 100 000 cells/mL. Neuronal cultures were allowed to grow for 8−10 days keeping in an incubator (Forma Direct Heat CO_2, Thermo Electron Corporation, Madrid, Spain) under saturated humidity at a partial pressure of 5% CO_2 in air at 37 °C. Once a dense neuronal network could be observed, motor cortex cultures were treated with the compounds **4**−**7(a,b)** at 100 μM, H_2O_2 (100 μM), or DMSO (1%) in order to evaluate their cytotoxic effects. After incubation for 24 h under the conditions described aboved, cell viability was evaluated using MTT as follows: 0.5 mg/mL MTT was added to each well, and incubation was performed at 37 °C for 2 h. Medium was removed, and formazan salt formed was dissolved in DMSO. The colorimetric determination was performed at 540 nm. Percent viability (% viability) was calculated as mean ± SEM of five determinations from five independent cultures.

ASSOCIATED CONTENT

Supporting Information

The Supporting Information is available free of charge at https://pubs.acs.org/doi/10.1021/acschemneuro.0c00687.

Copies of the 1D (^{1}H, ^{13}C{^{1}H}, DEPT-135) and 2D (COSY, HSQC) NMR spectra for all the compounds reported and details for the development of the ALLOPTML model (PDF)

Full lists of the values of MA and MMA, along with the data set used and the results of the MMA model for each case, including compound code, molecular descriptors, and the assay conditions (XLSX)

AUTHOR INFORMATION

Corresponding Authors

Ivo E. Sampaio-Dias − *LAQV/REQUIMTE, Dept. of Chemistry and Biochemistry, Faculty of Sciences, University of*

https://dx.doi.org/10.1021/acschemneuro.0c00687
ACS Chem. Neurosci. XXXX, XXX, XXX−XXX

Porto, 4169-007 Porto, Portugal; orcid.org/0000-0002-9071-6197; Email: idias@fc.up.pt

Xerardo García-Mera − *Dept. of Organic Chemistry, Faculty of Pharmacy, University of Santiago de Compostela, 15782 Santiago de Compostela, Spain*; Email: xerardo.garcia@usc.es

Humberto González-Díaz − *Dept. of Organic Chemistry II, University of Basque Country (UPV-EHU), 48940 Leioa, Spain; Basque Center for Biophysics (CSIC UPV/EHU), University of Basque Country (UPV-EHU), 48940 Leioa, Spain; IKERBASQUE, Basque Foundation for Science, 48011 Bilbao, Spain*; orcid.org/0000-0002-9392-2797; Email: humberto.gonzalezdiaz@ehu.es

Authors

José E. Rodríguez-Borges − *LAQV/REQUIMTE, Dept. of Chemistry and Biochemistry, Faculty of Sciences, University of Porto, 4169-007 Porto, Portugal*

Víctor Yáñez-Pérez − *Dept. of Organic Chemistry II, University of Basque Country (UPV-EHU), 48940 Leioa, Spain*

Sonia Arrasate − *Dept. of Pharmacology, Faculty of Medicine and Nursing, University of Basque Country (UPV-EHU), 48940 Leioa, Spain*; orcid.org/0000-0003-2601-5959

Javier Llorente − *Dept. of Pharmacology, Faculty of Medicine and Nursing, University of Basque Country (UPV-EHU), 48940 Leioa, Spain; Dept. of Pharmacology, University of Santiago de Compostela, 15782 Santiago de Compostela, Spain*

José M. Brea − *Innopharma Screening Platform, Biofarma Research group, Centre of Research in Molecular Medicine and Chronic Diseases CIMUS, University of Santiago de Compostela, 15782 Santiago de Compostela, Spain*

Harbil Bediaga − *Dept. of Organic Chemistry II, University of Basque Country (UPV-EHU), 48940 Leioa, Spain; Dept. of Physical Chemistry, University of Basque Country (UPV-EHU), 48940 Leioa, Spain*

Dolores Viña − *Dept. of Pharmacology, Faculty of Pharmacy and Centre of Research in Molecular Medicine and Chronic Diseases CIMUS, University of Santiago de Compostela, 15782 Santiago de Compostela, Spain*

María Isabel Loza − *Innopharma Screening Platform, Biofarma Research group, Centre of Research in Molecular Medicine and Chronic Diseases CIMUS, University of Santiago de Compostela, 15782 Santiago de Compostela, Spain*

Olga Caamaño − *Dept. of Organic Chemistry, Faculty of Pharmacy, University of Santiago de Compostela, 15782 Santiago de Compostela, Spain*

Complete contact information is available at: https://pubs.acs.org/10.1021/acschemneuro.0c00687

Author Contributions

I.E.S.-D. and H.G.-D. conceived and designed the experiments. I.E.S.-D. completed the experimental work. H.G.-D., S.A., J.L., V.Y.-P., and H.B. completed the development of the model. I.E.S.-D., X.G.-M., J.E.R.-B., H.G.-D., and O.C. analyzed the data. J.M.B. and M.I.L. completed the pharmacological assays. D.V. completed the biological assays. I.E.S.-D., X.G.-M., and H.G.-D. wrote the paper. All authors have given approval to the final version of the manuscript.

Funding

This research was funded by Fundação para a Ciência e Tecnologia (FCT, Portugal), through grants UIDB/50006/2020 (to LAQV-REQUIMTE Research Unit) and for project grants PTDC/BIA-MIB/29059/2017 and PEst-OE/QUI/UI0674/2013. This work was also supported by the Collaborative Project of Genomic Data Integration (CICLOGEN). The authors thank the USEF Drug Screening Platform at University of Santiago de Compostela for the support to carry out this work. The support of Ikerbasque, Basque Foundation for Science and the research grants from Ministry of Economy and Competitiveness, MINECO, Spain (FEDER CTQ2016−74881-P), and Basque government (IT1045−16) are also acknowledged. The financial support (ED431G 2019/02) from the Xunta de Galicia (Centro singular de investigación de Galicia accreditation 2019−2022) and the European Union (European Regional Development Fund—ERDF) is gratefully acknowledged. I.E.S.-D. thanks FCT for the doctoral grant SFRH/BD/93632/2013. X.G.-M. thanks Xunta de Galicia for financial support (GPC2014/003).

Notes

The authors declare no competing financial interest.

■ ACKNOWLEDGMENTS

Thanks are due to the Portuguese NMR network (RNRMN) for supporting the Laboratory for Structural Elucidation (LAE) of the Materials Centre of the University of Porto (CEMUP). I.E.S.-D. would like to thank Tiago Carrola for the valuable discussions about this work.

■ ABBREVIATIONS USED

^{13}C NMR, carbon-13 nuclear magnetic resonance; ^{1}H NMR, proton magnetic nuclear resonance; 2-Fu, 2-furoic acid; Ac, accuracy; BD, big data; CEMUP, Centro de Materiais da Universidade do Porto; CHO, Chinese hamster ovary cells; D_1R, dopamine D_1 receptor; DIEA, *N*-ethyl-*N*,*N*-diisopropylamine; DMSO, dimethyl sulfoxide; DMSO-d_6, deuterated dimethyl sulfoxide; DOS, diversity-oriented synthesis; ESI, electrospray ionization; GPCRs, G-protein-coupled receptors; HEK293, Human Embryonic Kidney 293 cells; HRMS, high-resolution mass spectrometry; LDA, Linear Discriminant Analysis; MA, moving average operators; mGluR, metabotropic glutamate receptor; MIF-1, Melanostatin; ML, machine learning; MMA, multiple moving average operators; NPA, *N*-propylapomorphine; PAM, positive allosteric modulator; PSA, polar surface area; PT, perturbation theory; PTML, perturbation theory and machine learning model; ROS, reactive oxygen species; Sn, sensitivity; Sp, specificity; TBTU, *O*-(benzotriazol-1-yl)-*N*,*N*,*N*′,*N*′-tetramethyluronium tetrafluoroborate; TLC, thin-layer chromatography; VCCLAB, Virtual Computational Chemistry Laboratory; WKY, Wistar-Kyoto

■ REFERENCES

(1) Mishra, A., Singh, S., and Shukla, S. (2018) Physiological and Functional Basis of Dopamine Receptors and Their Role in Neurogenesis: Possible Implication for Parkinson's disease. *J. Exp. Neurosci. 12*, 1−8.

(2) Beaulieu, J. M., and Gainetdinov, R. R. (2011) The physiology, signaling, and pharmacology of dopamine receptors. *Pharmacol. Rev. 63* (1), 182−217.

(3) Platania, C. B. M., Salomone, S., Leggio, G. M., Drago, F., and Bucolo, C. (2012) Homology modeling of dopamine D2 and D3 receptors: molecular dynamics refinement and docking evaluation. *PLoS One 7* (9), e44316.

(4) Lindgren, N., Usiello, A., Goiny, M., Haycock, J., Erbs, E., Greengard, P., Hokfelt, T., Borrelli, E., and Fisone, G. (2003) Distinct roles of dopamine D2L and D2S receptor isoforms in the regulation of

protein phosphorylation at presynaptic and postsynaptic sites. *Proc. Natl. Acad. Sci. U. S. A. 100* (7), 4305−4359.
(5) Nussinov, R., and Tsai, C. J. (2013) Allostery in disease and in drug discovery. *Cell 153* (2), 293−305.
(6) Khan, R. S., Yu, C., Kastin, A. J., He, Y., Ehrensing, R. H., Hsuchou, H., Stone, K. P., and Pan, W. (2010) Brain Activation by Peptide Pro-Leu-Gly-NH2 (MIF-1). *Int. J. Pept. 2010*, 537639.
(7) Allegretti, M., Cesta, M. C., and Locati, M. (2016) Allosteric Modulation of Chemoattractant Receptors. *Front. Immunol. 7*, 170.
(8) Verma, V., Mann, A., Costain, W., Pontoriero, G., Castellano, J. M., Skoblenick, K., Gupta, S. K., Pristupa, Z., Niznik, H. B., Johnson, R. L., Nair, V. D., and Mishra, R. K. (2005) Modulation of agonist binding to human dopamine receptor subtypes by L-prolyl-L-leucyl-glycinamide and a peptidomimetic analog. *J. Pharmacol. Exp. Ther. 315* (3), 1228−1236.
(9) Vartak, A. P., Skoblenick, K., Thomas, N., Mishra, R. K., and Johnson, R. L. (2007) Allosteric modulation of the dopamine receptor by conformationally constrained type VI beta-turn peptidomimetics of Pro-Leu-Gly-NH2. *J. Med. Chem. 50* (26), 6725−6729.
(10) Ferreira da Costa, J., Caamaño, O., Fernández, F., García-Mera, X., Sampaio-Dias, I. E., Brea, J. M., and Cadavid, M. I. (2013) Synthesis and allosteric modulation of the dopamine receptor by peptide analogs of l-prolyl-l-leucyl-glycinamide (PLG) modified in the l-proline or l-proline and l-leucine scaffolds. *Eur. J. Med. Chem. 69* (SupplementC), 146−158.
(11) Sampaio-Dias, I. E., Silva-Reis, S. C., García-Mera, X., Brea, J., Loza, M. I., Alves, C. S., Algarra, M., and Rodríguez-Borges, J. E. (2019) Synthesis, Pharmacological, and Biological Evaluation of MIF-1 Picolinoyl Peptidomimetics as Positive Allosteric Modulators of D2R. *ACS Chem. Neurosci. 10* (8), 3690−3702.
(12) Sampaio-Dias, I. E., Sousa, C. A. D., Garcia-Mera, X., Ferreira da Costa, J., Caamano, O., and Rodriguez-Borges, J. E. (2016) *Org. Biomol. Chem. 14*, 11065−11069.
(13) Celis, M. E., Taleisnik, S., and Walter, R. (1971) Regulation of formation and proposed structure of the factor inhibiting the release of melanocyte-stimulating hormone. *Proc. Natl. Acad. Sci. U. S. A. 68* (7), 1428−1433.
(14) Srivastava, L. K., Bajwa, S. B., Johnson, R. L., and Mishra, R. K. (1988) Interaction of l-Prolyl-l-Leucyl Glycinamide with Dopamine D2 Receptor: Evidence for Modulation of Agonist Affinity States in Bovine Striatal Membranes. *J. Neurochem. 50* (3), 960−968.
(15) Chiu, S., Paulose, C. S., and Mishra, R. K. (1981) Effect of L-prolyl-L-leucyl-glycinamide (PLG) on neuroleptic-induced catalepsy and dopamine/neuroleptic receptor bindings. *Peptides 2* (1), 105−111.
(16) Saitton, S., Del Tredici, A. L., Mohell, N., Vollinga, R. C., Boström, D., Kihlberg, J., and Luthman, K. (2004) Design, synthesis and evaluation of a PLG tripeptidomimetic based on a pyridine scaffold. *J. Med. Chem. 47* (26), 6595−6602.
(17) Reed, G. W., Olson, G. A., and Olson, R. D. (1994) The Tyr-MIF-1 family of peptides. *Neurosci. Biobehav. Rev. 18* (4), 519−525.
(18) Mishra, R. K., Makman, M. H., Costain, W. J., Nair, V. D., and Johnson, R. L. (1999) Modulation of agonist stimulated adenylyl cyclase and GTPase activity by L-pro-L-leu-glycinamide and its peptidomimetic analogue in rat striatal membranes. *Neurosci. Lett. 269* (1), 21−24.
(19) Birtwistle, J., and Baldwin, D. (1998) Role of dopamine in schizophrenia and Parkinson's disease. *Br. J. Nurs. 7* (14), 832−834. 836, 838−841.
(20) Smith, J. R., and Morgan, M. (1982) The effects of prolyl-leucyl-glycine amide on drug-induced rotation in lesioned rats. *Gen. Pharmacol. 13* (3), 203−207.
(21) Marcotte, E. R., Chugh, A., Mishra, R. K., and Johnson, R. L. (1998) Protection Against MPTP Treatment by an Analog of Pro-Leu-Gly-NH2 (PLG, MIF-1). *Peptides 19* (2), 403−406.
(22) Barbeau, A., Roy, M., and Kastin, A. J. (1976) Double-blind evaluation of oral L-prolyl-Lleucyl-glycine amide in Parkinson's disease. *Can. Med. Assoc. J. 114* (2), 120−122.
(23) Sharma, S., Paladino, P., Gabriele, J., Saeedi, H., Henry, P., Chang, M., Mishra, R. K., and Johnson, R. L. (2003) Pro-Leu-glycinamide and its peptidomimetic, PAOPA, attenuate haloperidol induced vacuous chewing movements in rat: A model of human tardive dyskinesia. *Peptides 24* (2), 313−319.
(24) Mycroft, F. J., Bhargava, H. N., and Wei, E. T. (1987) Pharmacological activities of the MIF-1 analogues Pro-Leu-Gly, Tyr-Pro-Leu-Gly and pareptide. *Peptides 8* (6), 1051−1055.
(25) Chiu, P., Rajakumar, G., Chiu, S., Johnson, R. L., and Mishra, R. K. (1985) Mesolimbic and striatal dopamine receptor supersensitivity: Prophylactic and reversal effects of L-prolyl-L-leucyl-glycinamide (PLG). *Peptides 6* (2), 179−183.
(26) Reed, L. L., and Johnson, P. L. (1973) Solid state conformation of the C-terminal tripeptide of oxytocin, L-Pro-L-Leu-Gly-NH2.0.5H2O. *J. Am. Chem. Soc. 95* (22), 7523−7524.
(27) Aizpurua, J. M., Palomo, C., Balentová, E., Jimenez, A., Andreieff, E., Sagartzazu-Aizpurua, M., Miranda, J. I., and Linden, A. (2013) Chirality-Driven Folding of Short β-Lactam Pseudopeptides. *J. Org. Chem. 78* (2), 224−237.
(28) Johnson, R. L., Rajakumar, G., Yu, K. L., and Mishra, R. K. (1986) Synthesis of Pro-Leu-Gly-NH2 analogues modified at the prolyl residue and evaluation of their effects on the receptor binding activity of the central dopamine receptor agonist, ADTN. *J. Med. Chem. 29* (10), 2104−2107.
(29) Sampaio-Dias, I. E., Sousa, C. A. D., Silva-Reis, S. C., Ribeiro, S., García-Mera, X., and Rodríguez-Borges, J. E. (2017) Highly efficient one-pot assembly of peptides by double chemoselective coupling. *Org. Biomol. Chem. 15* (36), 7533−7542.
(30) Liang, X., Haynes, B. S., and Montoya, A. (2018) Acid-Catalyzed Ring Opening of Furan in Aqueous Solution. *Energy Fuels 32* (4), 4139−4148.
(31) Open-source cheminformatics, http://zinc15.docking.org/patterns/home (accessed 2020-07-10).
(32) Christopoulos, A., and Kenakin, T. (2002) G protein-coupled receptor allosterism and complexing. *Pharmacol. Rev. 54* (2), 323−374.
(33) Bhagwanth, S., Mishra, R. K., and Johnson, R. L. (2013) Development of peptidomimetic ligands of Pro-Leu-Gly-NH(2) as allosteric modulators of the dopamine D(2) receptor. *Beilstein J. Org. Chem. 9*, 204−214.
(34) Alonso, N., Caamano, O., Romero-Duran, F. J., Luan, F., Cordeiro, M. N. D. S., Yanez, M., Gonzalez-Diaz, H., and Garcia-Mera, X. (2013) Model for High-Throughput Screening of Multitarget Drugs in Chemical Neurosciences: Synthesis, Assay, and Theoretic Study of Rasagiline Carbamates. *ACS Chem. Neurosci. 4* (10), 1393−1403.
(35) Luan, F., Cordeiro, M. N. D. S., Alonso, N., García-Mera, X., Caamaño, O., Romero-Duran, F. J., Yañez, M., and González-Díaz, H. (2013) TOPS-MODE model of multiplexing neuroprotective effects of drugs and experimental-theoretic study of new 1,3-rasagiline derivatives potentially useful in neurodegenerative diseases. *Bioorg. Med. Chem. 21* (7), 1870−1879.
(36) Ricart, K. C., and Fiszman, M. L. (2001) Hydrogen Peroxide-Induced Neurotoxicity in Cultured Cortical Cells Grown in Serum-Free and Serum-Containing Media. *Neurochem. Res. 26* (7), 801−808.
(37) Schneider, G. (2011) Computational medicinal chemistry. *Future Med. Chem. 3* (4), 393−394.
(38) Csermely, P., Nussinov, R., and Szilagyi, A. (2013) From allosteric drugs to allo-network drugs: state of the art and trends of design, synthesis and computational methods. *Curr. Top. Med. Chem. 13* (1), 2−4.
(39) Szilagyi, A., Nussinov, R., and Csermely, P. (2013) Allo-network drugs: extension of the allosteric drug concept to protein- protein interaction and signaling networks. *Curr. Top. Med. Chem. 13* (1), 64−77.
(40) Csermely, P., Korcsmaros, T., Kiss, H. J., London, G., and Nussinov, R. (2013) Structure and dynamics of molecular networks: a novel paradigm of drug discovery: a comprehensive review. *Pharmacol. Ther. 138* (3), 333−408.
(41) Taylor, P. J. (1990) *Comprehensive Medicinal Chemistry*, 1990 ed., Vol. *4*, p 241−294, Pergamon Press, Oxford.
(42) Wang, J., Yun, D., Yao, J., Fu, W., Huang, F., Chen, L., Wei, T., Yu, C., Xu, H., Zhou, X., Huang, Y., Wu, J., Qiu, P., and Li, W. (2018)

https://dx.doi.org/10.1021/acschemneuro.0c00687
ACS Chem. Neurosci. XXXX, XXX, XXX−XXX

Design, synthesis and QSAR study of novel isatin analogues inspired Michael acceptor as potential anticancer compounds. *Eur. J. Med. Chem. 144*, 493−503.

(43) Pogorzelska, A., Sławiński, J., Żołnowska, B., Szafrański, K., Kawiak, A., Chojnacki, J., Ulenberg, S., Zielińska, J., and Bączek, T. (2017) Novel 2-(2-alkylthiobenzenesulfonyl)-3-(phenylprop-2-ynylideneamino)guanidine derivatives as potent anticancer agents - Synthesis, molecular structure, QSAR studies and metabolic stability. *Eur. J. Med. Chem. 138*, 357−370.

(44) Sławiński, J., Szafrański, K., Pogorzelska, A., Żołnowska, B., Kawiak, A., Macur, K., Belka, M., and Bączek, T. (2017) Novel 2-benzylthio-5-(1,3,4-oxadiazol-2-yl)benzenesulfonamides with anticancer activity: Synthesis, QSAR study, and metabolic stability. *Eur. J. Med. Chem. 132*, 236−248.

(45) Murahari, M., Kharkar, P. S., Lonikar, N., and Mayur, Y. C. (2017) Design, synthesis, biological evaluation, molecular docking and QSAR studies of 2,4-dimethylacridones as anticancer agents. *Eur. J. Med. Chem. 130*, 154−170.

(46) Ruddarraju, R. R., Murugulla, A. C., Kotla, R., Chandra Babu Tirumalasetty, M., Wudayagiri, R., Donthabakthuni, S., Maroju, R., Baburao, K., and Parasa, L. S. (2016) Design, synthesis, anticancer, antimicrobial activities and molecular docking studies of theophylline containing acetylenes and theophylline containing 1,2,3-triazoles with variant nucleoside derivatives. *Eur. J. Med. Chem. 123*, 379−396.

(47) Singh, H., Kumar, R., Singh, S., Chaudhary, K., Gautam, A., and Raghava, G. P. (2016) Prediction of anticancer molecules using hybrid model developed on molecules screened against NCI-60 cancer cell lines. *BMC Cancer 16*, 77.

(48) Pingaew, R., Prachayasittikul, V., Worachartcheewan, A., Nantasenamat, C., Prachayasittikul, S., Ruchirawat, S., and Prachayasittikul, V. (2015) Novel 1,4-naphthoquinone-based sulfonamides: Synthesis, QSAR, anticancer and antimalarial studies. *Eur. J. Med. Chem. 103*, 446−459.

(49) Anwer, Z., and Gupta, S. P. (2013) A QSAR study on some series of anticancer tyrosine kinase inhibitors. *Med. Chem. (Sharjah, United Arab Emirates) 9* (2), 203−212.

(50) Toropov, A. A., Toropova, A. P., Benfenati, E., Gini, G., Leszczynska, D., and Leszczynski, J. (2011) SMILES-based QSAR approaches for carcinogenicity and anticancer activity: comparison of correlation weights for identical SMILES attributes. *Anti-Cancer Agents Med. Chem. 11* (10), 974−982.

(51) Huang, X. Y., Shan, Z. J., Zhai, H. L., Li, L. N., and Zhang, X. Y. (2011) Molecular design of anticancer drug leads based on three-dimensional quantitative structure-activity relationship. *J. Chem. Inf. Model. 51* (8), 1999−2006.

(52) Benfenati, E., Toropov, A. A., Toropova, A. P., Manganaro, A., and Gonella Diaza, R. (2011) coral Software: QSAR for Anticancer Agents. *Chem. Biol. Drug Des. 77* (6), 471−476.

(53) González-Díaz, H., Bonet, I., Terán, C., De Clercq, E., Bello, R., García, M. M., Santana, L., and Uriarte, E. (2007) ANN-QSAR model for selection of anticancer leads from structurally heterogeneous series of compounds. *Eur. J. Med. Chem. 42* (5), 580−585.

(54) González-Díaz, H., Viña, D., Santana, L., de Clercq, E., and Uriarte, E. (2006) Stochastic entropy QSAR for the in silico discovery of anticancer compounds: prediction, synthesis, and in vitro assay of new purine carbanucleosides. *Bioorg. Med. Chem. 14* (4), 1095−1107.

(55) González-Díaz, H., Gia, O., Uriarte, E., Hernádez, I., Ramos, R., Chaviano, M., Seijo, S., Castillo, J. A., Morales, L., Santana, L., Akpaloo, D., Molina, E., Cruz, M., Torres, L. A., and Cabrera, M. A. (2003) Markovian chemicals "in silico" design (MARCH-INSIDE), a promising approach for computer-aided molecular design I: discovery of anticancer compounds. *J. Mol. Model. 9* (6), 395−407.

(56) Jung, M., Kim, H., and Kim, M. (2003) Chemical genomics strategy for the discovery of new anticancer agents. *Curr. Med. Chem. 10* (9), 757−762.

(57) Shi, L. M., Fan, Y., Myers, T. G., O'Connor, P. M., Paull, K. D., Friend, S. H., and Weinstein, J. N. (1998) Mining the NCI anticancer drug discovery databases: genetic function approximation for the QSAR study of anticancer ellipticine analogues. *J. Chem. Inf. Comput. Sci. 38* (2), 189−199.

(58) Han, L., Cui, J., Lin, H., Ji, Z., Cao, Z., Li, Y., and Chen, Y. (2006) Recent progresses in the application of machine learning approach for predicting protein functional class independent of sequence similarity. *Proteomics 6* (14), 4023−4037.

(59) Chou, K. C., and Shen, H. B. (2010) Plant-mPLoc: a top-down strategy to augment the power for predicting plant protein subcellular localization. *PLoS One 5* (6), e11335.

(60) Chou, K. C., and Shen, H. B. (2008) Cell-PLoc: a package of Web servers for predicting subcellular localization of proteins in various organisms. *Nat. Protoc. 3* (2), 153−162.

(61) Cai, Y. D., and Chou, K. C. (2005) Predicting enzyme subclass by functional domain composition and pseudo amino acid composition. *J. Proteome Res. 4* (3), 967−971.

(62) Shen, H. B., and Chou, K. C. (2009) QuatIdent: a web server for identifying protein quaternary structural attribute by fusing functional domain and sequential evolution information. *J. Proteome Res. 8* (3), 1577−1584.

(63) Chou, K. C., and Shen, H. B. (2006) Large-scale predictions of gram-negative bacterial protein subcellular locations. *J. Proteome Res. 5* (12), 3420−3428.

(64) Rodriguez-Soca, Y., Munteanu, C. R., Dorado, J., Pazos, A., Prado-Prado, F. J., and González-Díaz, H. (2010) Trypano-PPI: a web server for prediction of unique targets in trypanosome proteome by using electrostatic parameters of protein-protein interactions. *J. Proteome Res. 9* (2), 1182−1190.

(65) Munteanu, C. R., Vázquez, J. M., Dorado, J., Sierra, A. P., Sánchez-González, A., Prado-Prado, F. J., and González-Díaz, H. (2009) Complex network spectral moments for ATCUN motif DNA cleavage: first predictive study on proteins of human pathogen parasites. *J. Proteome Res. 8* (11), 5219−5228.

(66) González-Díaz, H., Saiz-Urra, L., Molina, R., Santana, L., and Uriarte, E. (2007) A model for the recognition of protein kinases based on the entropy of 3D van der Waals interactions. *J. Proteome Res. 6* (2), 904−908.

(67) González-Díaz, H., Prado-Prado, F., García-Mera, X., Alonso, N., Abeijón, P., Caamaño, O., Yañez, M., Munteanu, C. R., Pazos, A., Dea-Ayuela, M. A., Gómez-Muñoz, M. T., Garijo, M. M., Sansano, J., and Ubeira, F. M. (2011) MIND-BEST: Web server for drugs and target discovery; design, synthesis, and assay of MAO-B inhibitors and theoretical-experimental study of G3PDH protein from Trichomonas gallinae. *J. Proteome Res. 10* (4), 1698−1718.

(68) Concu, R., Dea-Ayuela, M. A., Perez-Montoto, L. G., Bolas-Fernández, F., Prado-Prado, F. J., Podda, G., Uriarte, E., Ubeira, F. M., and González-Díaz, H. (2009) Prediction of enzyme classes from 3D structure: a general model and examples of experimental-theoretic scoring of peptide mass fingerprints of Leishmania proteins. *J. Proteome Res. 8* (9), 4372−4382.

(69) Agüero-Chapin, G., Varona-Santos, J., de la Riva, G. A., Antunes, A., González-Villa, T., Uriarte, E., and González-Díaz, H. (2009) Alignment-free prediction of polygalacturonases with pseudofolding topological indices: experimental isolation from Coffea arabica and prediction of a new sequence. *J. Proteome Res. 8* (4), 2122−2128.

(70) Martínez-Arzarte, S. G., Tenorio-Borroto, E., Pliego, A. B., Díaz-Albiter, H. M., Vázquez-Chagoyán, J. C., and González-Díaz, H. (2017) PTML Model for Proteome Mining of B-cell Epitopes and Theoretic-Experimental Study of Bm86 Protein Sequences from Colima, Mexico. *J. Proteome Res. 16* (11), 4093−4103.

(71) Fernández, M., Caballero, F., Fernández, L., Abreu, J. I., and Acosta, G. (2008) Classification of conformational stability of protein mutants from 3D pseudo-folding graph representation of protein sequences using support vector machines. *Proteins: Struct., Funct., Genet. 70* (1), 167−175.

(72) Fernández, L., Caballero, J., Abreu, J. I., and Fernández, M. (2007) Amino Acid Sequence Autocorrelation Vectors and Bayesian-Regularized Genetic Neural Networks for Modeling Protein Conformational Stability: Gene V Protein Mutants. *Proteins: Struct., Funct., Genet. 67*, 834−852.

https://dx.doi.org/10.1021/acschemneuro.0c00687
ACS Chem. Neurosci. XXXX, XXX, XXX−XXX

(73) Caballero, J., Fernández, L., Abreu, J. I., and Fernández, M. (2006) Amino Acid Sequence Autocorrelation vectors and ensembles of Bayesian-Regularized Genetic Neural Networks for prediction of conformational stability of human lysozyme mutants. *J. Chem. Inf. Model. 46* (3), 1255−1268.

(74) Perez-Riverol, Y., Audain, E., Millan, A., Ramos, Y., Sanchez, A., Vizcaíno, J. A., Wang, R., Müller, M., Machado, Y. J., Betancourt, L. H., González, L. J., Padrón, G., and Besada, V. (2012) Isoelectric point optimization using peptide descriptors and support vector machines. *J. Proteomics 75* (7), 2269−2274.

(75) Greener, J. G., and Sternberg, M. J. E. (2015) AlloPred: prediction of allosteric pockets on proteins using normal mode perturbation analysis. *BMC Bioinf. 16*, 335.

(76) Gaulton, A., Hersey, A., Nowotka, M., Bento, A. P., Chambers, J., Mendez, D., Mutowo, P., Atkinson, F., Bellis, L. J., Cibrián-Uhalte, E., Davies, M., Dedman, N., Karlsson, A., Magariños, M. P., Overington, J. P., Papadatos, G., Smit, I., and Leach, A. R. (2017) The ChEMBL database in 2017. *Nucleic Acids Res. 45* (D1), D945.

(77) Gaulton, A., Bellis, L. J., Bento, A. P., Chambers, J., Davies, M., Hersey, A., Light, Y., McGlinchey, S., Michalovich, D., Al-Lazikani, B., and Overington, J. P. (2012) ChEMBL: a large-scale bioactivity database for drug discovery. *Nucleic Acids Res. 40* (D1), D1100−D1107.

(78) González-Díaz, H., Arrasate, S., Gómez-SanJuan, A., Sotomayor, N., Lete, E., Besada-Porto, L., and Ruso, J. M. (2013) General Theory for Multiple Input-Output Perturbations in Complex Molecular Systems. 1. Linear QSPR Electronegativity Models in Physical, Organic, and Medicinal Chemistry. *Curr. Top. Med. Chem. 13* (14), 1713−1741.

(79) Blázquez-Barbadillo, C., Aranzamendi, E., Coya, E., Lete, E., Sotomayor, N., and González-Díaz, H. (2016) Perturbation theory model of reactivity and enantioselectivity of palladium-catalyzed Heck-Heck cascade reactions. *RSC Adv. 6* (45), 38602−38610.

(80) Casañola-Martin, G. M., Le-Thi-Thu, H., Pérez-Giménez, F., Marrero-Ponce, Y., Merino-Sanjuán, M., Abad, C., and González-Díaz, H. (2016) Multi-output Model with Box-Jenkins Operators of Quadratic Indices for Prediction of Malaria and Cancer Inhibitors Targeting Ubiquitin-Proteasome Pathway (UPP) Proteins. *Curr. Protein Pept. Sci. 17* (3), 220−227.

(81) Romero-Durán, F. J., Alonso, N., Yañez, M., Caamaño, O., García-Mera, X., and González-Díaz, H. (2016) Brain-inspired cheminformatics of drug-target brain interactome, synthesis, and assay of TVP1022 derivatives. *Neuropharmacology 103*, 270−278.

(82) Kleandrova, V. V., Luan, F., González-Díaz, H., Ruso, J. M., Speck-Planche, A., and Cordeiro, M. N. D. S. (2014) Computational Tool for Risk Assessment of Nanomaterials: Novel QSTR-Perturbation Model for Simultaneous Prediction of Ecotoxicity and Cytotoxicity of Uncoated and Coated Nanoparticles under Multiple Experimental Conditions. *Environ. Sci. Technol. 48* (24), 14686−14694.

(83) Luan, F., Kleandrova, V. V., González-Díaz, H., Ruso, J. M., Melo, A., Speck-Planche, A., and Cordeiro, M. N. D. S. (2014) Computer-aided nanotoxicology: assessing cytotoxicity of nanoparticles under diverse experimental conditions by using a novel QSTR-perturbation approach. *Nanoscale 6* (18), 10623−10630.

(84) Speck-Planche, A., and Cordeiro, M. N. D. S. (2017) Fragment-based in silico modeling of multi-target inhibitors against breast cancer-related proteins. *Mol. Diversity 21* (3), 511−523.

(85) Speck-Planche, A., Kleandrova, V. V., Luan, F., and Cordeiro, M. N. D. S. (2013) Unified multi-target approach for the rational in silico design of anti-bladder cancer agents. *Anti-Cancer Agents Med. Chem. 13* (5), 791−800.

(86) Speck-Planche, A., Kleandrova, V. V., Luan, F., and Cordeiro, M. N. D. S. (2012) Chemoinformatics in multi-target drug discovery for anti-cancer therapy: in silico design of potent and versatile anti-brain tumor agents. *Anti-Cancer Agents Med. Chem. 12* (6), 678−685.

(87) Speck-Planche, A., Kleandrova, V. V., Luan, F., and Cordeiro, M. N. D. S. (2012) Rational drug design for anti-cancer chemotherapy: multi-target QSAR models for the in silico discovery of anti-colorectal cancer agents. *Bioorg. Med. Chem. 20* (15), 4848−4855.

(88) Speck-Planche, A., Kleandrova, V. V., Luan, F., and Cordeiro, M. N. D. S. (2012) Chemoinformatics in anti-cancer chemotherapy: multi-target QSAR model for the in silico discovery of anti-breast cancer agents. *Eur. J. Pharm. Sci. 47* (1), 273−279.

(89) Cordeiro, M. N. D. S., and Speck-Planche, A. (2013) Computer-aided drug design, synthesis and evaluation of new anti-cancer drugs. *Curr. Top. Med. Chem. 12* (24), 2703−2704.

(90) Speck-Planche, A., Kleandrova, V. V., Luan, F., and Cordeiro, M. N. D. S. (2011) Multi-target drug discovery in anti-cancer therapy: fragment-based approach toward the design of potent and versatile anti-prostate cancer agents. *Bioorg. Med. Chem. 19* (21), 6239−6244.

(91) Speck-Planche, A., and Cordeiro, M. N. D. S. (2017) Advanced In Silico Approaches for Drug Discovery: Mining Information from Multiple Biological and Chemical Data Through mtk- QSBER and pt-QSPR Strategies. *Curr. Med. Chem. 24*, 1687−1704.

(92) Collier, G., and Ortiz, V. (2013) Emerging computational approaches for the study of protein allostery. *Arch. Biochem. Biophys. 538* (1), 6−15.

(93) Marrero-Ponce, Y., Siverio-Mota, D., Gálvez-Llompart, M., Recio, M. C., Giner, R. M., García-Domènech, R., Torrens, F., Arán, V. J., Cordero-Maldonado, M. L., Esguera, C. V., de Witte, P. A., and Crawford, A. D. (2011) Discovery of novel anti-inflammatory drug-like compounds by aligning in silico and in vivo screening: the nitroindazolinone chemotype. *Eur. J. Med. Chem. 46* (12), 5736−5753.

(94) Tetko, I. V., Gasteiger, J., Todeschini, R., Mauri, A., Livingstone, D., Ertl, P., Palyulin, V. A., Radchenko, E. V., Zefirov, N. S., Makarenko, A. S., Tanchuk, V. Y., and Prokopenko, V. V. (2005) Virtual computational chemistry laboratory − design and description. *J. Comput.-Aided Mol. Des. 19* (6), 453−463.

(95) Gottlieb, H. E., Kotlyar, V., and Nudelman, A. (1997) NMR Chemical Shifts of Common Laboratory Solvents as Trace Impurities. *J. Org. Chem. 62* (21), 7512−7515.

https://dx.doi.org/10.1021/acschemneuro.0c00687
ACS Chem. Neurosci. XXXX, XXX, XXX−XXX